

Making sense of all that AVO and inversion stuff!

The Milton Dobrin Lecture
April, 2010

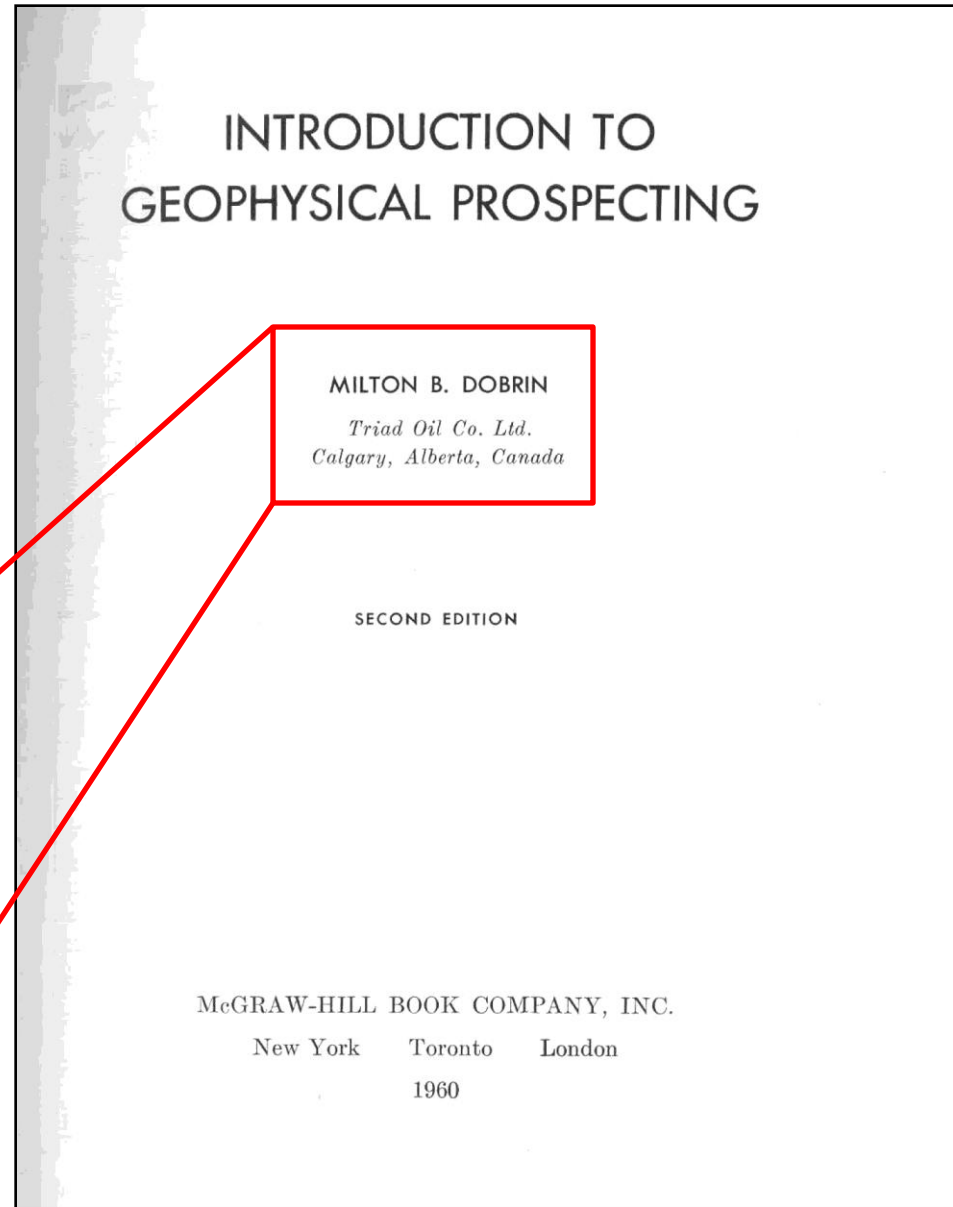
Brian Russell
Hampson-Russell,
A CGGVeritas Company



Milton B. Dobrin

Born: April 7, 1915, in Vancouver

A gifted teacher, best known for his influential book on geophysical exploration: editions 1 and 2 written in Calgary, edition 3 written in Houston, where he was a Professor at U of H.

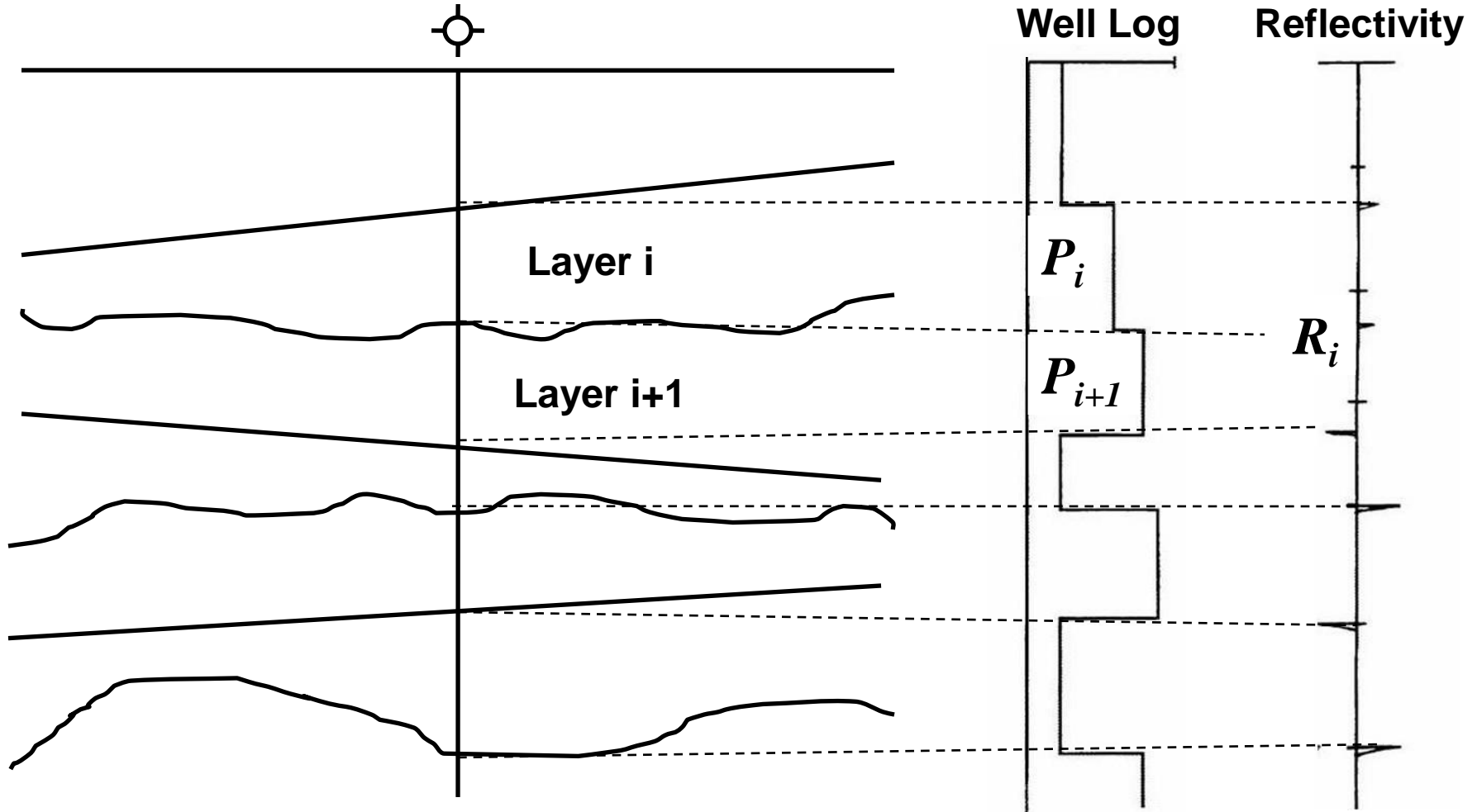


MILTON B. DOBRIN
Triad Oil Co. Ltd.
Calgary, Alberta, Canada

Died: May 22, 1980, in Houston.

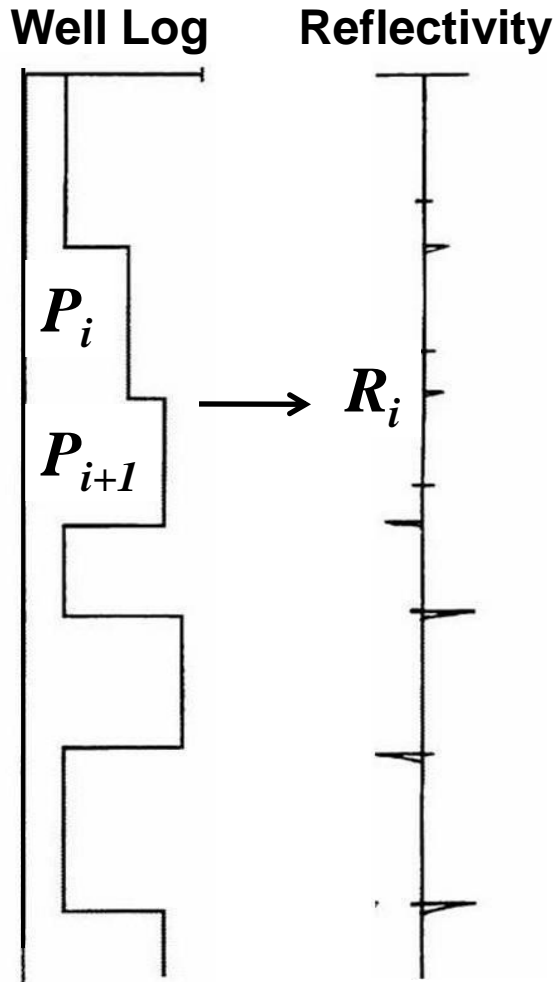
- The Amplitude Variations with Offset (AVO) technique has grown to include a multitude of sub-techniques, each with its own assumptions.
- AVO techniques can be subdivided as either:
 - (1) seismic reflectivity or (2) impedance methods.
- Seismic reflectivity methods include: Near and Far stacks, Intercept vs Gradient analysis and the fluid factor.
- Impedance methods include: P and S-impedance inversion, Lambda-mu-rho, Elastic Impedance and Poisson Impedance.
- The objective of this talk is to make sense of all of these methods and show how they are related.
- Let us start by looking at the different ways in which a geologist and geophysicist look at data.

From Geology to Geophysics



For a layered earth, a well log measures a parameter P for each layer and the seismic trace measures the interface reflectivity R .

The reflectivity



The reflectivity at each interface is found by dividing the change in the value of the parameter by twice its average.

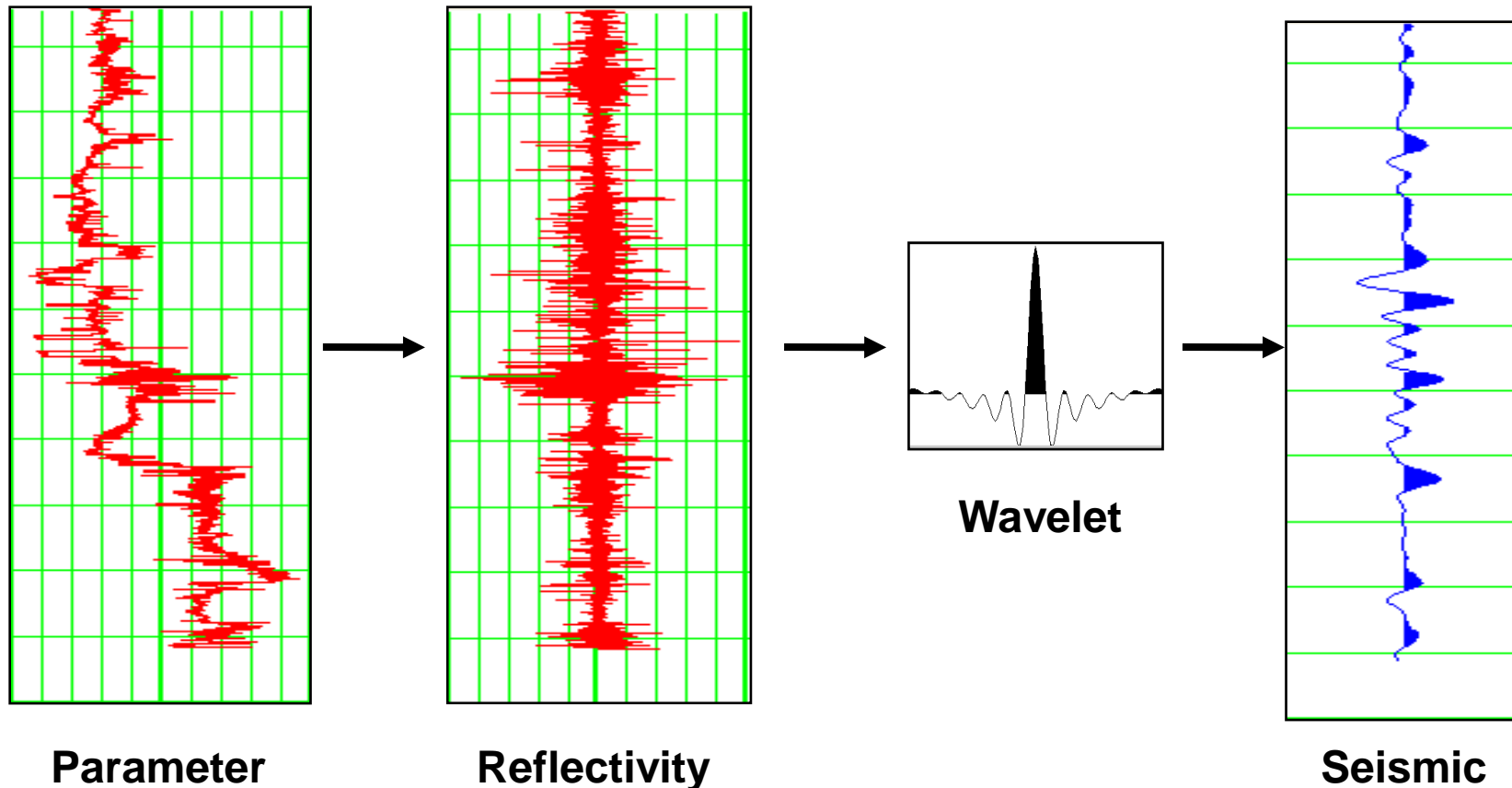
As an equation, this is written:

$$R_i = \frac{P_{i+1} - P_i}{P_{i+1} + P_i} = \frac{\Delta P_i}{2\bar{P}_i},$$

where :

$$\Delta P_i = P_{i+1} - P_i \text{ and } \bar{P}_i = \frac{P_{i+1} + P_i}{2}$$

The convolutional model



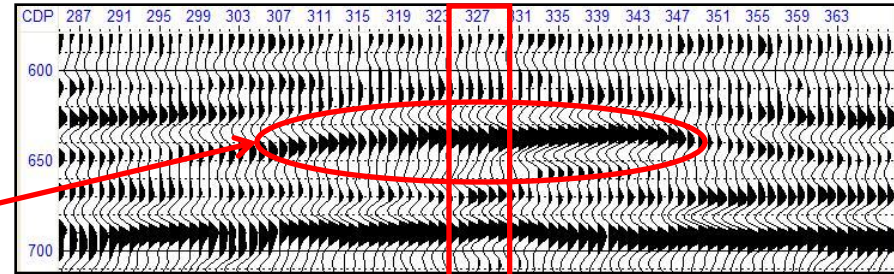
One extra thing to observe is that the seismic trace is the convolution of the reflectivity with a wavelet ($S = W * R$).

Which parameter?

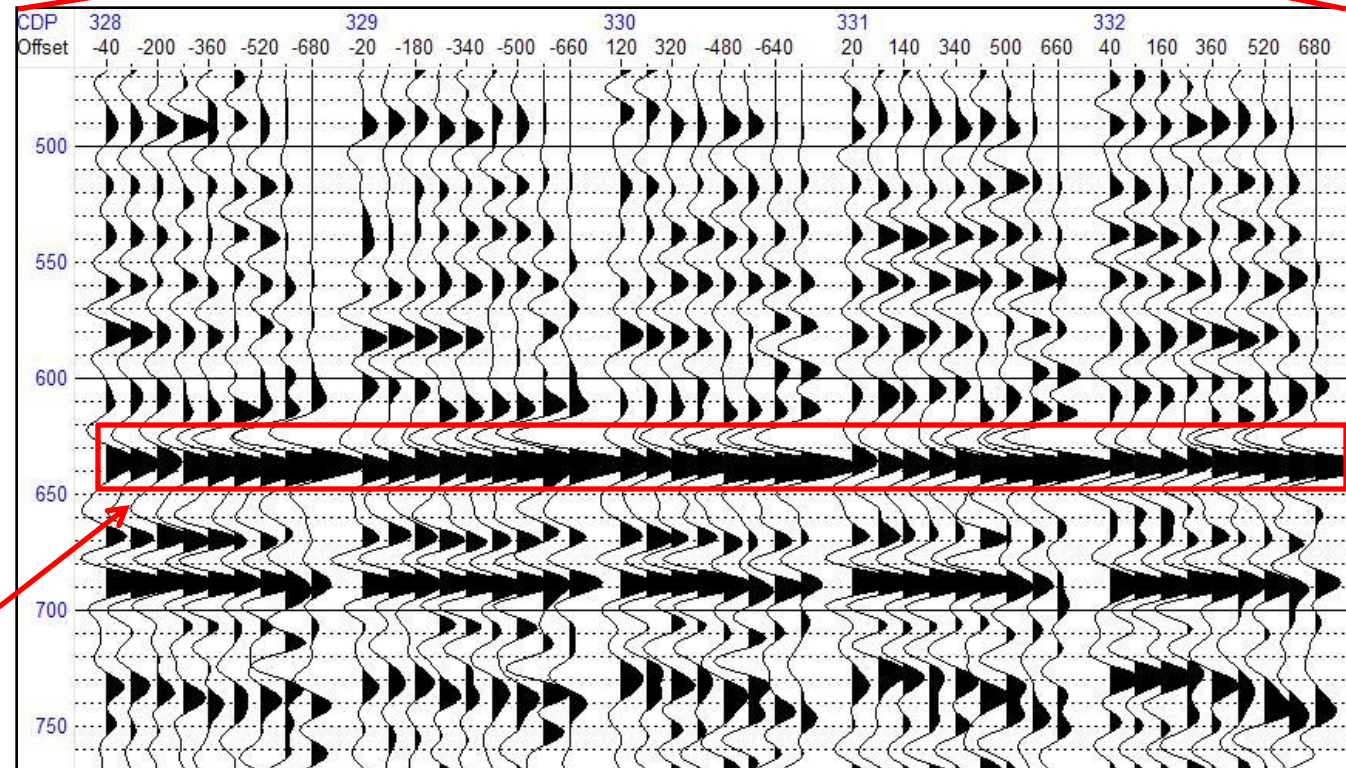
- But which parameter P are we interested in?
- To the geophysicist the choices usually are:
 - P-wave velocity (V_P)
 - S-wave velocity (V_S)
 - Density (ρ)
 - Transforms of velocity and density such as acoustic impedance (ρV_P) and shear impedance (ρV_S).
- The geologist would add:
 - Gamma ray
 - Water saturation, etc...
- How many of these can we derive from the seismic?
- Let us start by looking at a seismic example.

A Seismic Example

Here is a portion of a 2D seismic line showing a gas sand “bright-spot”.

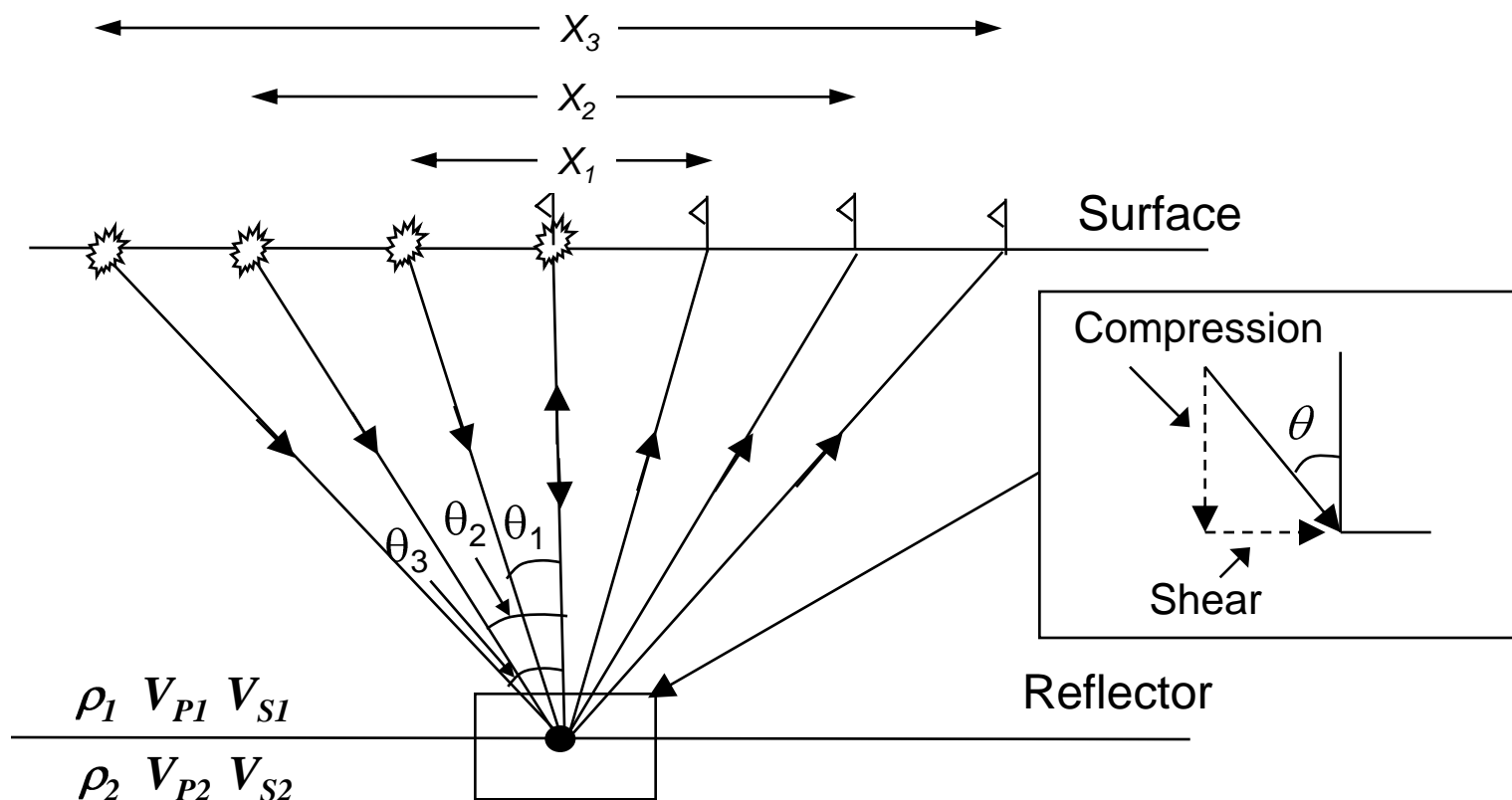


The seismic line is the “stack” of a series of CMP gathers, as shown here.



The gas sand is a typical Class 3 AVO anomaly.

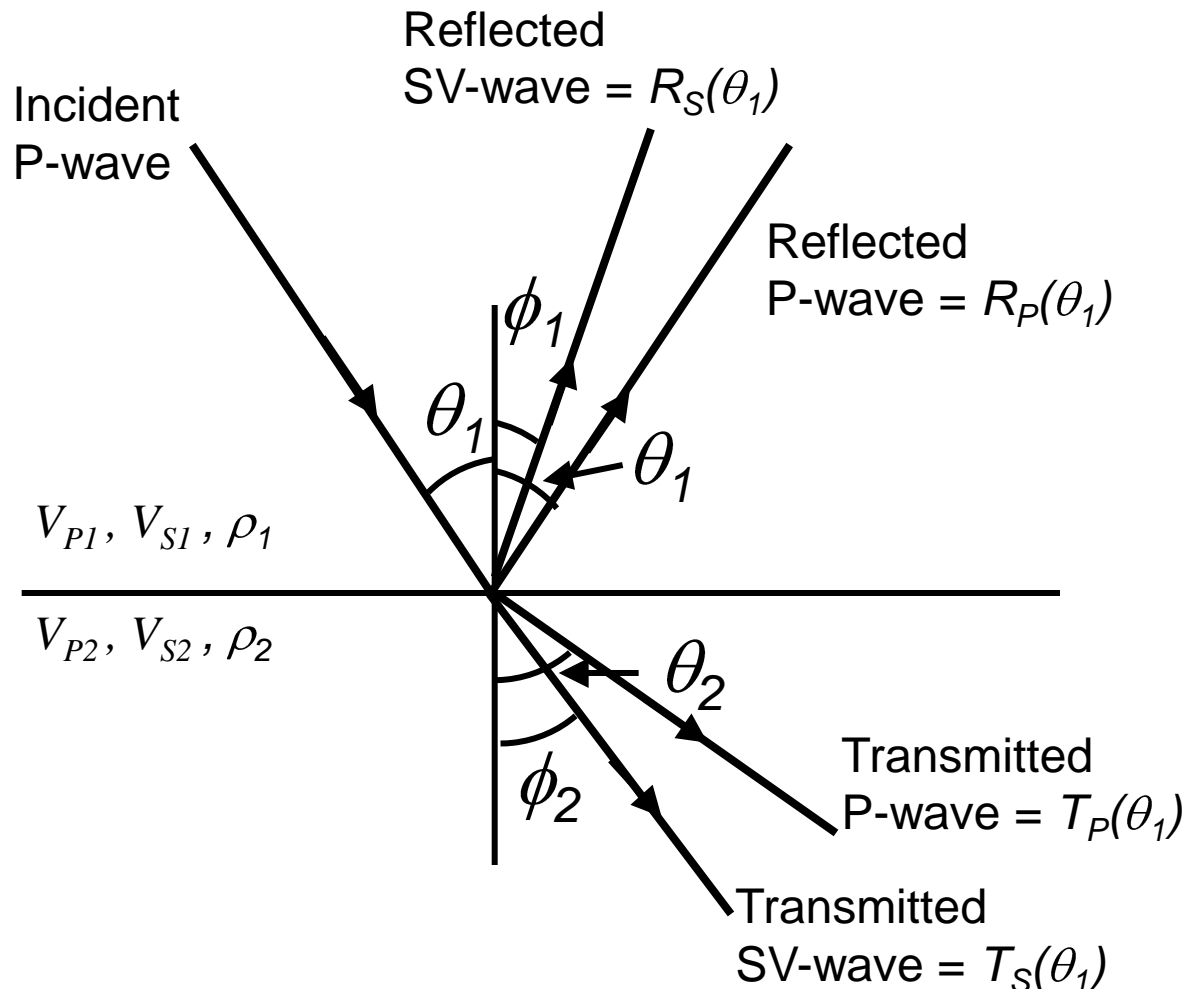
The pre-stack gathers



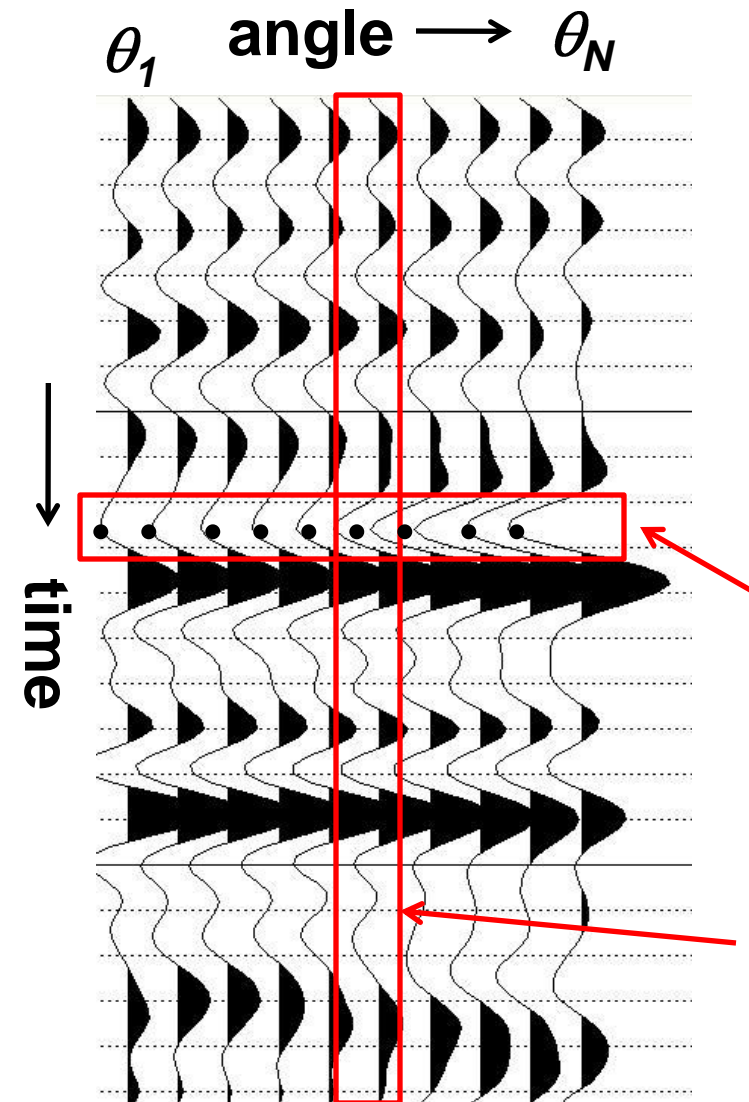
- The traces in a seismic gather reflect from the subsurface at increasing angles of incidence θ , related to offset X .
- If the angle is greater than zero, notice that there is both a shear component and a compressional component.

Mode Conversion of an incident P-Wave

More technically speaking, if $\theta > 0$, an incident *P*-wave will produce both *P* and *SV* reflected and transmitted waves. This is called *mode conversion*.



The angle gather



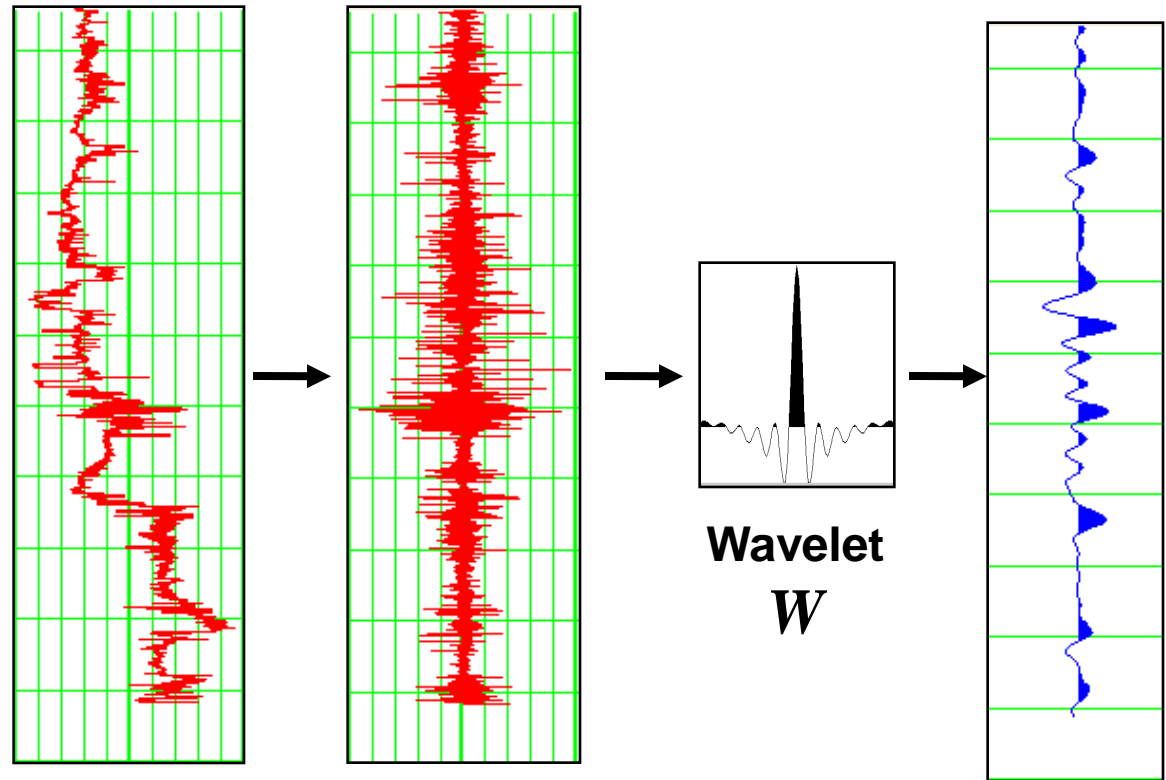
Using the P-wave velocity, we can transform the offset gathers shown earlier to angle gathers. There are two ways in which AVO methods extract reflectivity from angle gathers.

We can perform a least-squares fit to the reflectivity at a given time for all angles.

Or we can extract the reflectivity function at a single angle θ .

The zero-angle model

The zero-angle trace can be modeled using a well known model, where the trace is the convolution of the acoustic impedance reflectivity with the wavelet.



Acoustic
Impedance

Reflectivity

Wavelet
 W

Seismic

Note: the stack is only approximately zero-angle.

$$AI = \rho V_P \Rightarrow R_{AI} = \frac{\Delta AI}{2AI} \Rightarrow S = W * R_{AI}$$

The Aki-Richards equation

- Any other angle is modelled with the Aki-Richards equation, a linearized form of the Zoeppritz equations which is written (and is the basis of virtually all AVO methods):

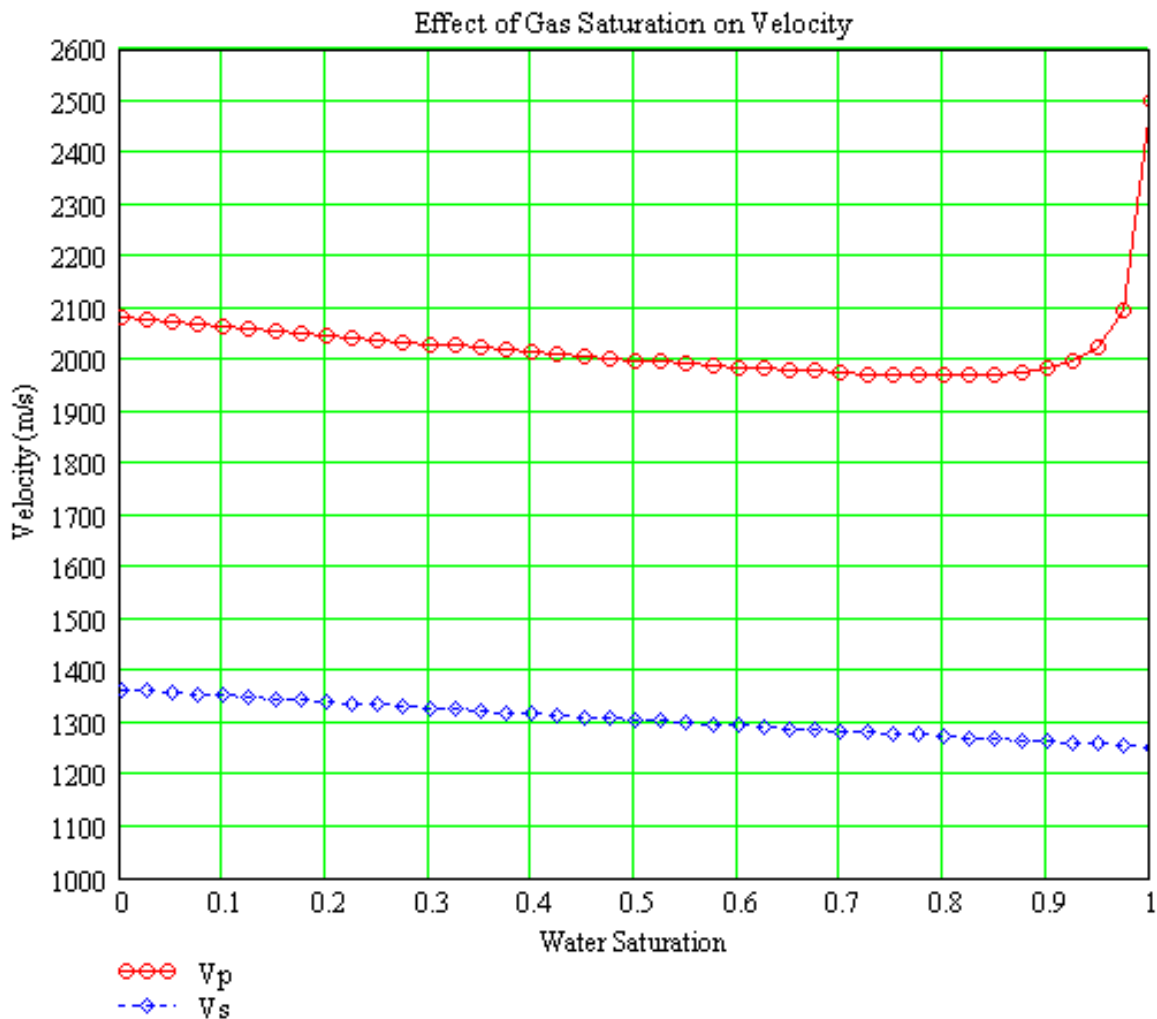
$$R(\theta) = aR_{VP} + bR_{VS} + cR_D,$$

$$\text{where : } R_{VP} = \frac{\Delta V_P}{2\bar{V}_P}, R_{VS} = \frac{\Delta V_S}{2\bar{V}_S}, R_D = \frac{\Delta\rho}{2\bar{\rho}},$$

$$a = 1 + \tan^2 \theta, b = -8K \sin^2 \theta, c = 1 - 4K \sin^2 \theta, \text{ and } K = \left(\frac{\bar{V}_S}{\bar{V}_P} \right)^2.$$

- The Aki-Richards equation says that the reflectivity at angle θ is the weighted sum of the V_P , V_S and density reflectivities.

S-wave Velocity



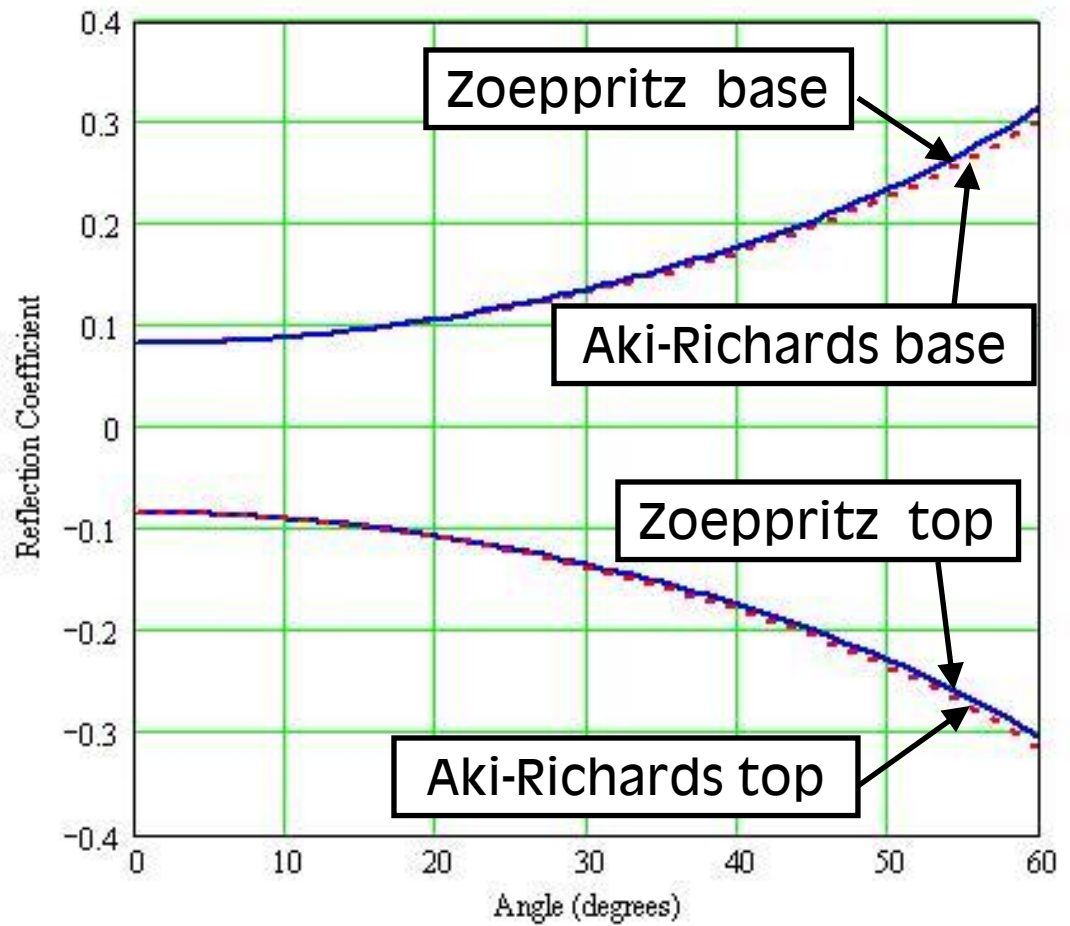
The reason that S-wave velocity has such an impact on interpretation is shown on the left, where P and S-wave velocity are shown as a function of gas saturation in the reservoir.

Note that P-wave velocity drops dramatically, but S-wave velocity only increases slightly.

AVO Curves

This figure on the right shows AVO curves computed using the Zoeppritz equations and the Aki-Richards equation for the top and base of a gas sand model.

Notice that the fit is quite good in this case.



The Fatti et al. Equation

- To show the connection between the pre- and post-stack formulations more clearly, Fatti et al. (1994) re-formulated the Aki-Richards equation as:

$$R_P(\theta) = aR_{AI} + bR_{SI} + c'R_D,$$

where $R_{AI} = \frac{\Delta AI}{2AI} = R_{VP} + R_D$, $AI = \rho V_P$,

$$R_{SI} = \frac{\Delta SI}{2SI} = R_{VS} + R_D, SI = \rho V_S,$$

and $c' = 4K \sin^2 \theta - \tan^2 \theta$.

- Notice that $R_P(0) = R_{AI}$, equal to the zero-angle model.

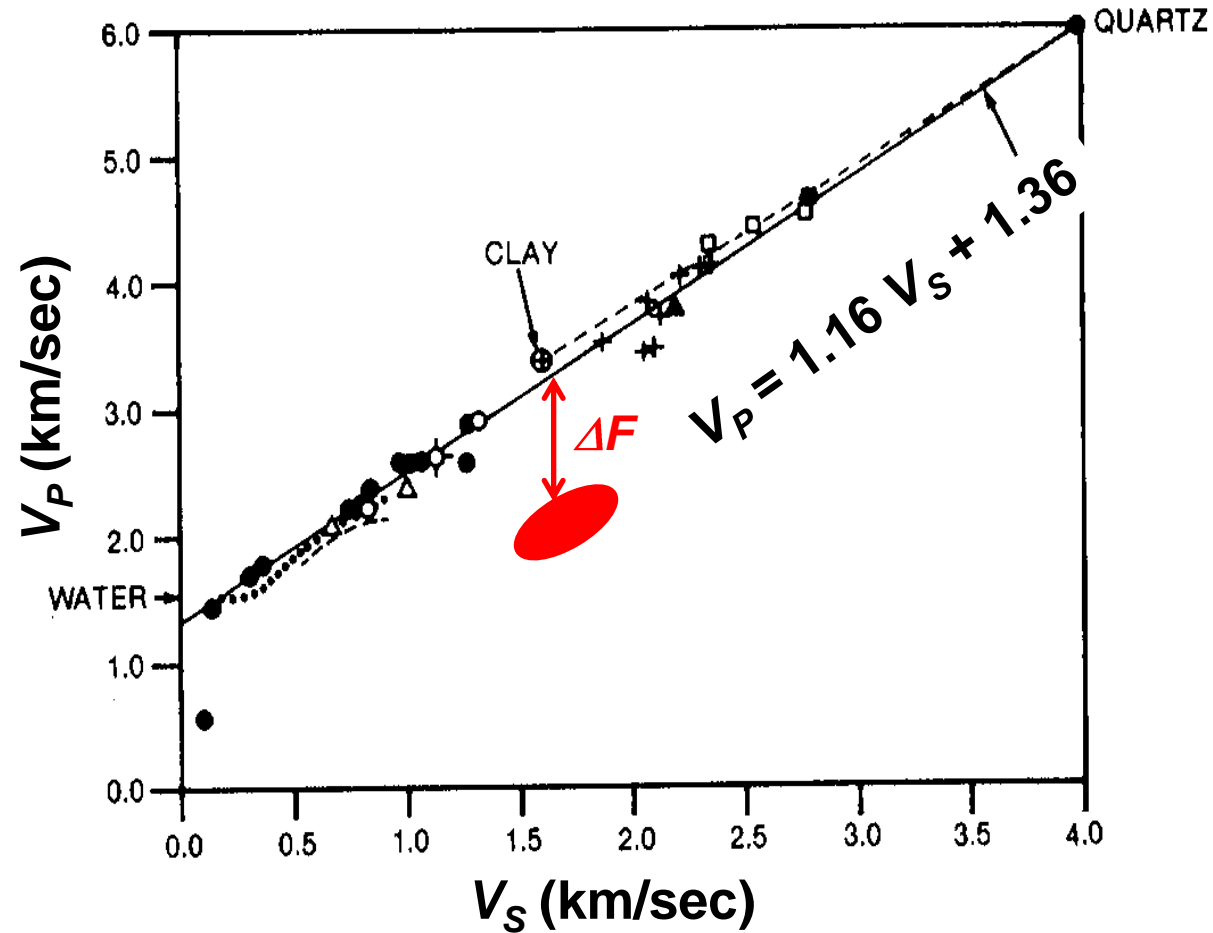
- Fatti et al. (1994) is a refinement of the original work of Smith and Gidlow (1987).
- The key difference between the two papers is the Smith and Gidlow use the original Aki-Richards equation and absorb density into V_P using Gardner's equation.
- Both papers also define the Poisson's Ratio reflectivity R_σ and the fluid factor ΔF (which was derived from Castagna's mudrock line) as:

$$R_\sigma = \frac{\Delta \sigma}{2 \bar{\sigma}} = R_{AI} - R_{SI}, \text{ and}$$

$$\Delta F = R_{AI} - g R_{SI}, \text{ where } g = 1.16(V_S / V_P)$$

The Mudrock Line

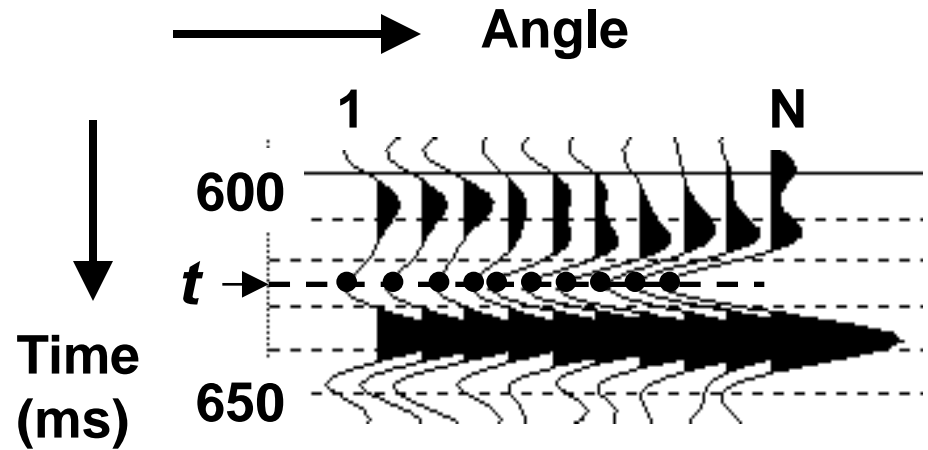
In non-mathematical terms, Fatti and Smith define ΔF as the difference away from the V_P versus V_S line that defines wet sands and shales. These differences should indicate fluid anomalies.



Modified from Castagna et al, (1985)

Estimating R_{AI} and R_{SI}

To estimate the reflectivities, the amplitudes at each time t in an N -trace angle gather are picked as shown here.



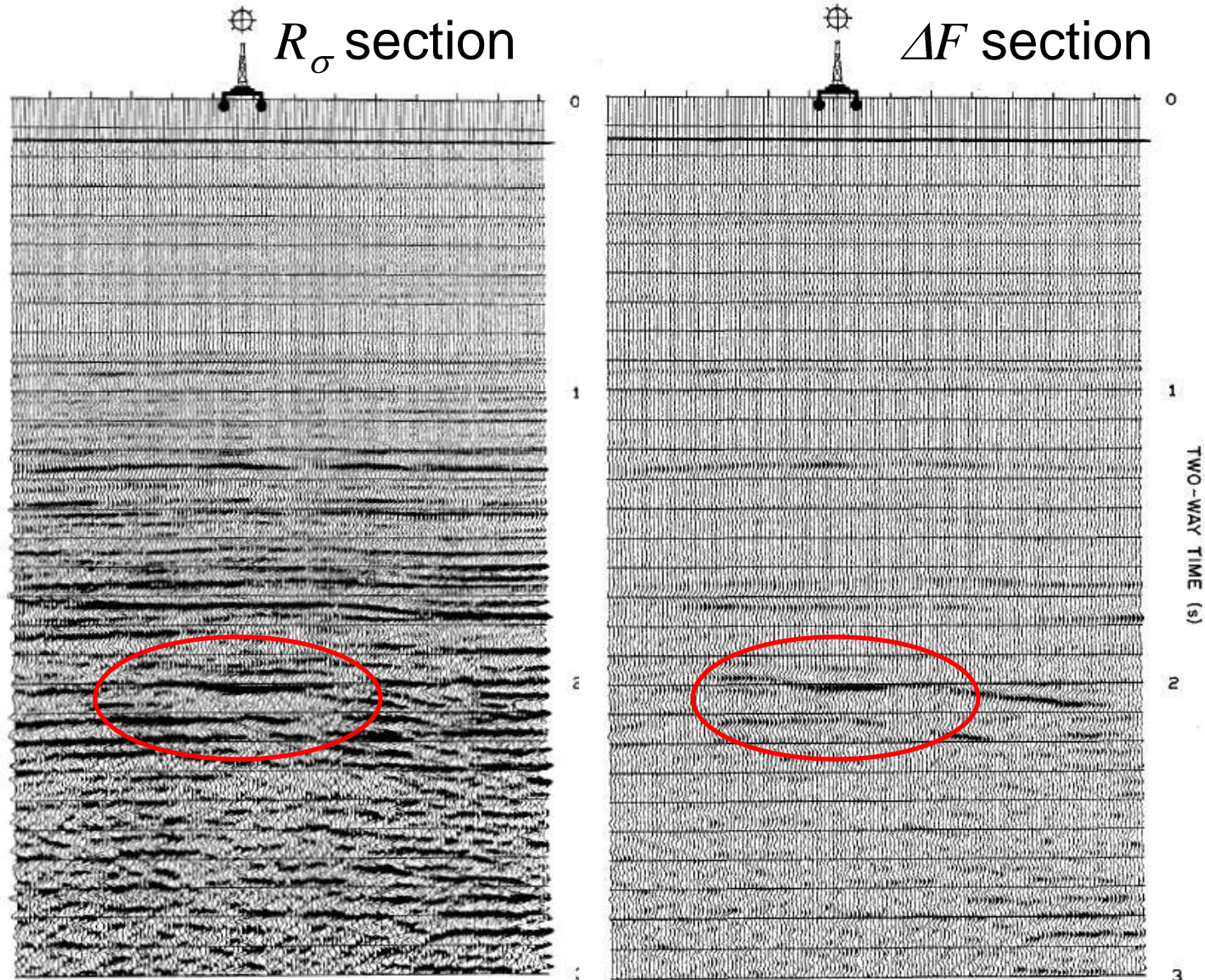
Generalized inverse of weight matrix

We can solve for the reflectivities at each time sample using least-squares:

$$\underbrace{\begin{bmatrix} R_{AI} \\ R_{SI} \\ R_D \end{bmatrix}}_{\text{Reflectivities}} = \underbrace{\begin{bmatrix} \text{weight} \\ \text{matrix} \end{bmatrix}^{-1}}_{\text{Generalized inverse of weight matrix}} \underbrace{\begin{bmatrix} R_P(\theta_1) \\ \vdots \\ R_P(\theta_N) \end{bmatrix}}_{\text{Observations}}$$

Smith and Gidlow's results

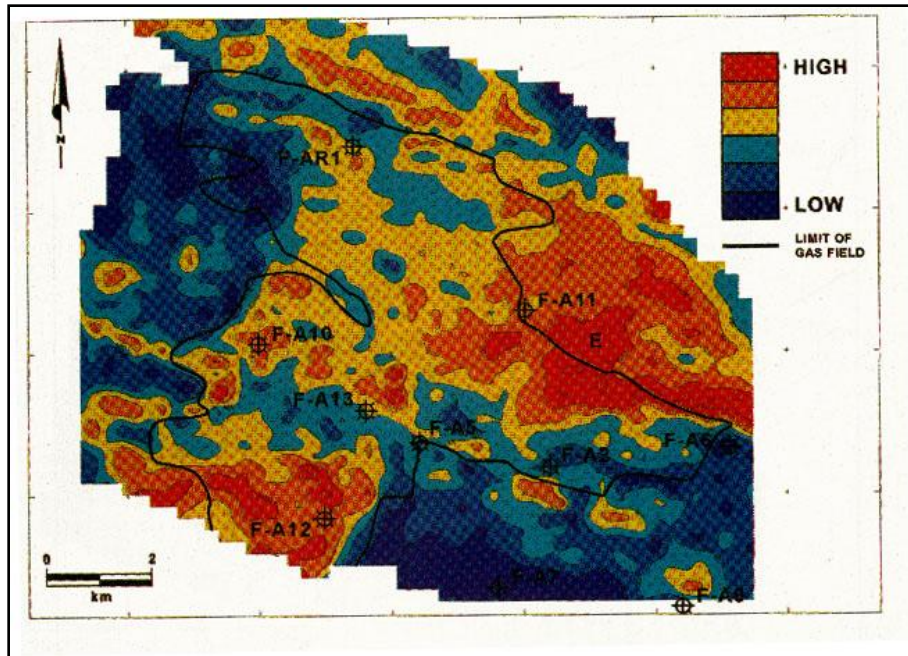
Here are the R_σ and ΔF sections from an offshore field in South Africa. Note that the fluid factor ΔF shows the fluid anomaly the best.



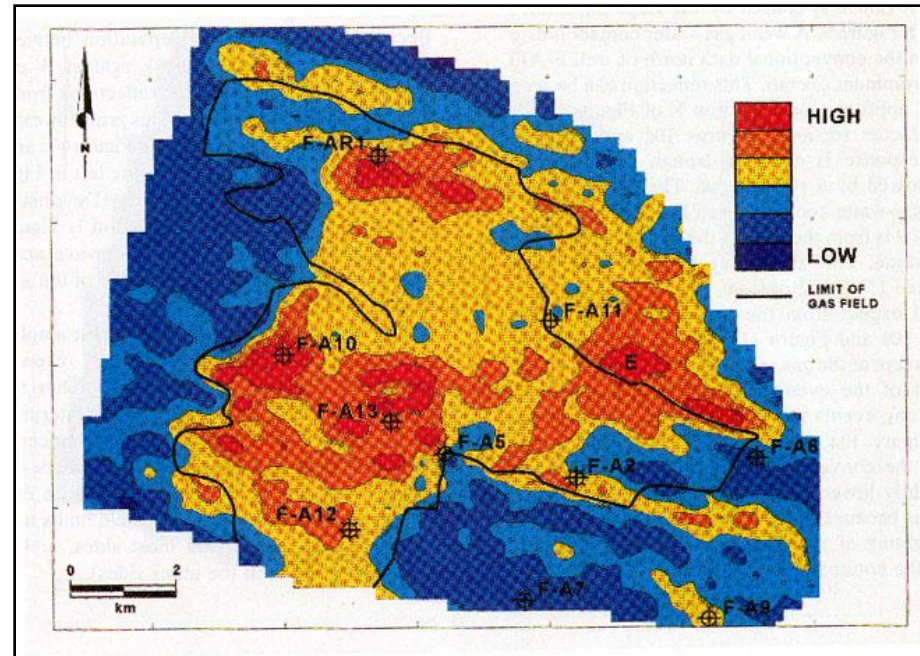
Smith and Gidlow
(1987)

Fatti et al.'s results

Seismic Amplitude Map



ΔF Map



Fatti et al. (1994)

A comparison of a seismic amplitude map and a fluid factor map for a gas sand play. Note the correlation of high ΔF values with the gas wells.

- Another approach to AVO is the Intercept/Gradient method, which involves re-arranging the Aki-Richards equation to:

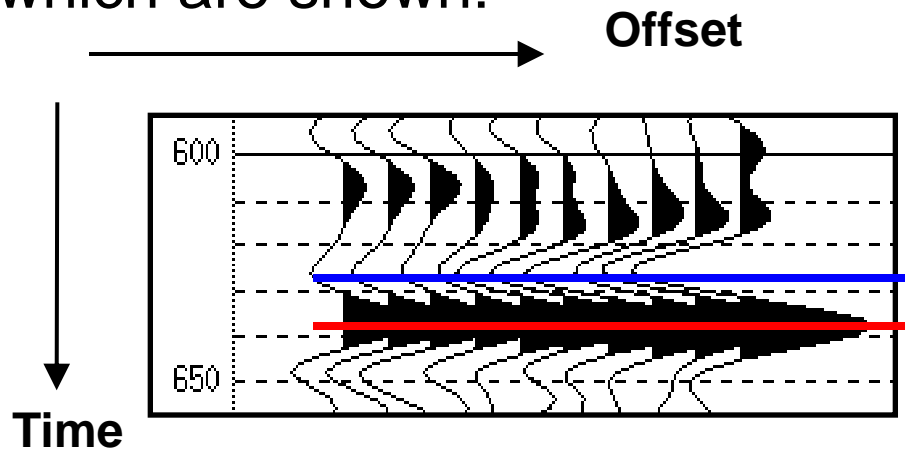
$$R_P(\theta) = R_{AI} + G \sin^2 \theta + R_{VP} \sin^2 \theta \tan^2 \theta, \text{ where :}$$

$$G = R_{VP} - 8KR_{VS} - 4KR_D = \text{the gradient.}$$

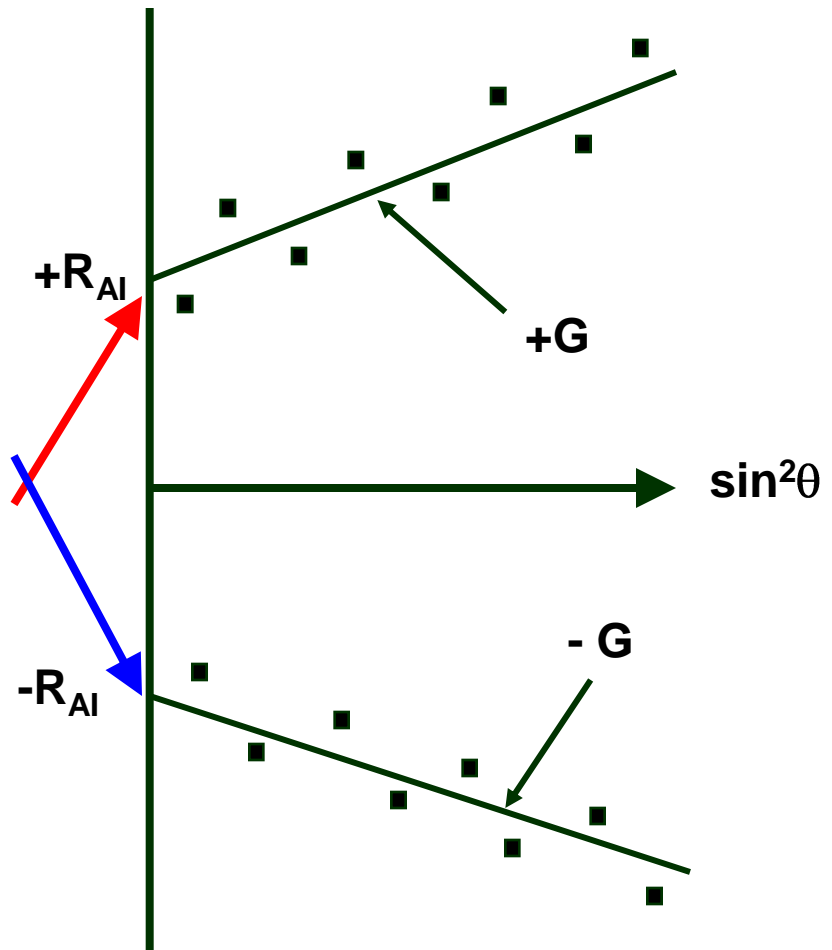
- This is again a weighted reflectivity equation with weights of $a = 1$, $b = \sin^2 \theta$, $c = \sin^2 \theta \tan^2 \theta$.
- The three reflectivities are usually called A , B , and C (or: intercept, gradient and curvature) but this obscures the fact that only G is a new reflectivity compared with the previous methods.

The Intercept/Gradient method

Again, the amplitudes are extracted at all times, two of which are shown:

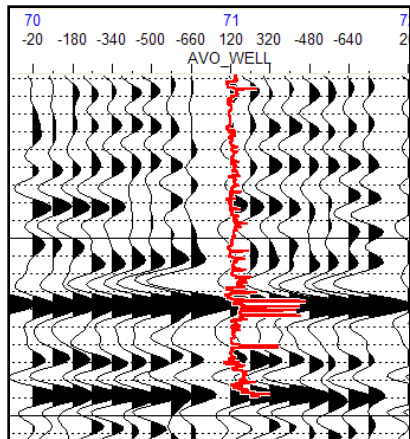
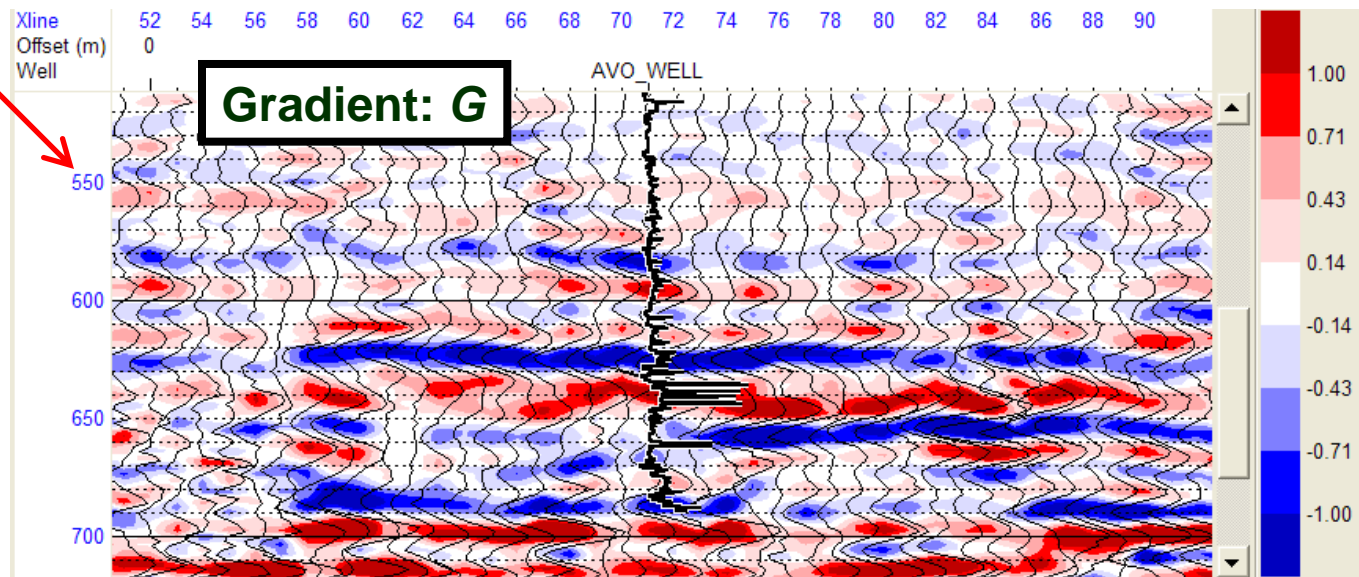
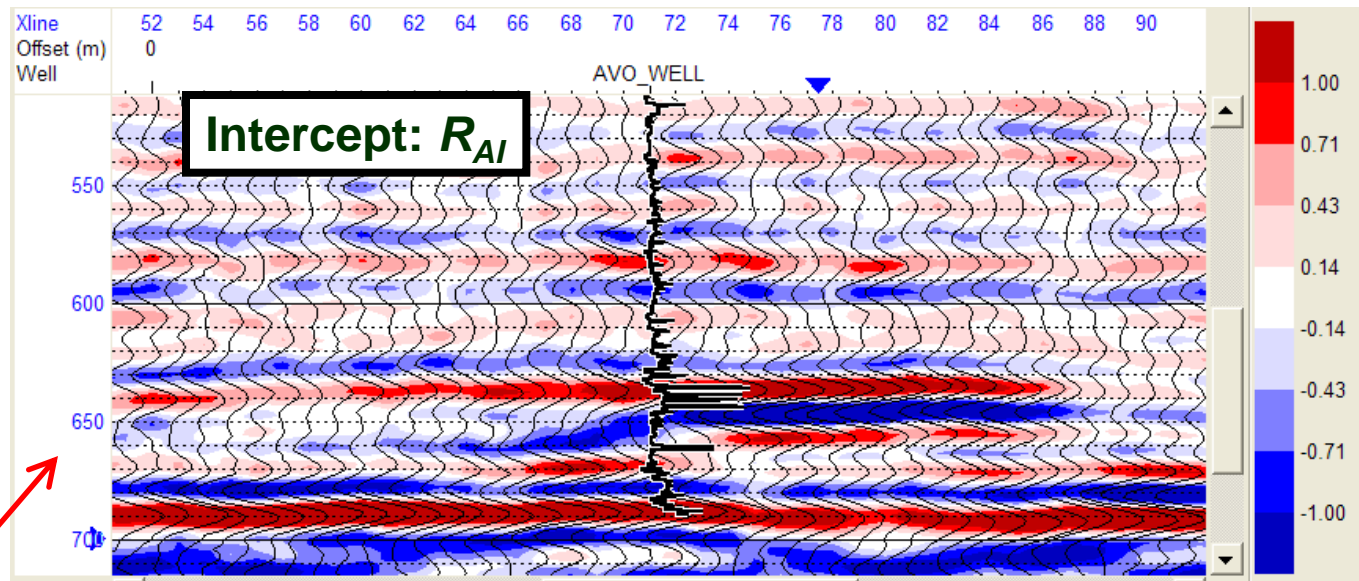


The Aki-Richards equation predicts a linear relationship between these amplitudes and $\sin^2\theta$. Regression curves are calculated to give R_{AI} and G values for each time sample.



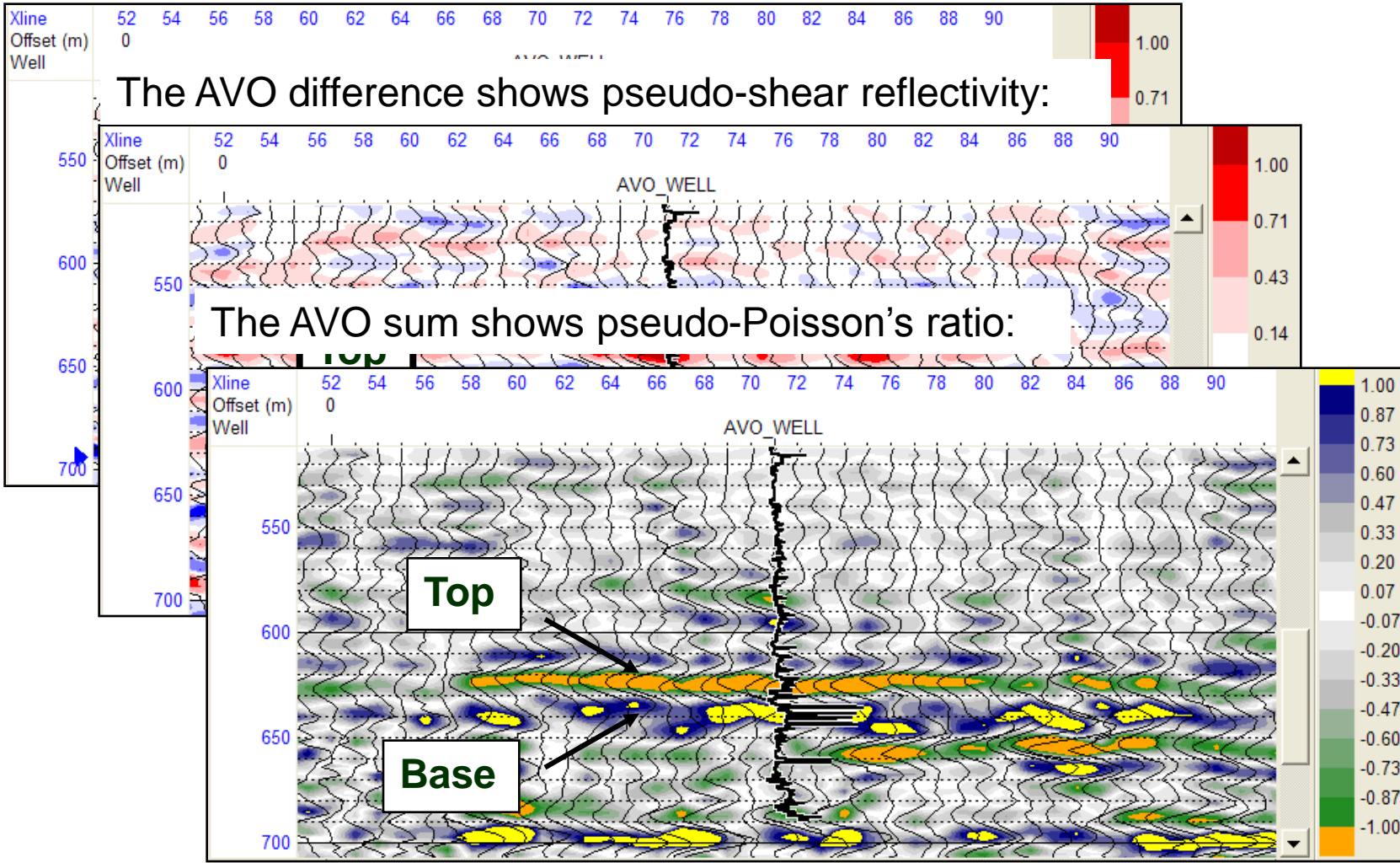
The Intercept/Gradient method

The result of this calculation is to produce 2 basic attribute volumes

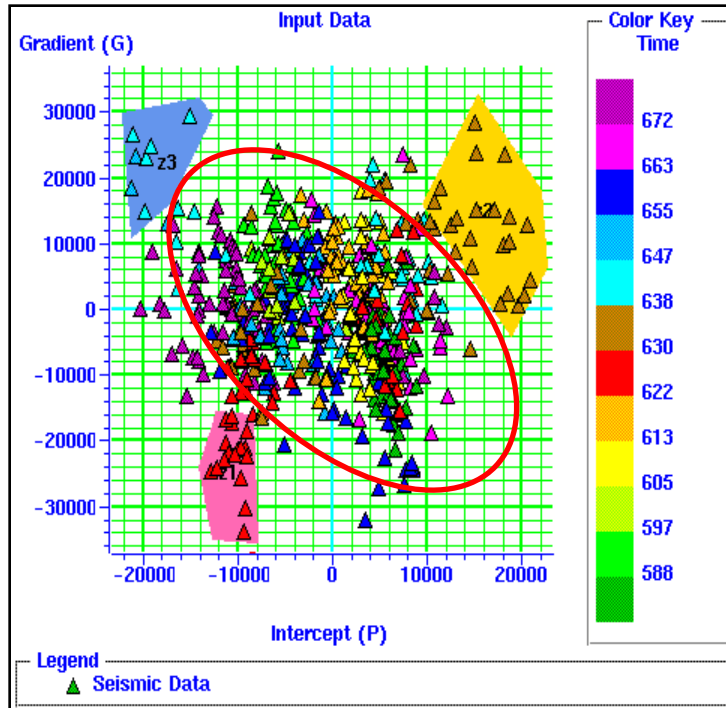


Intercept/Gradient combinations

The AVO product shows a positive response at the top and base of the reservoir:



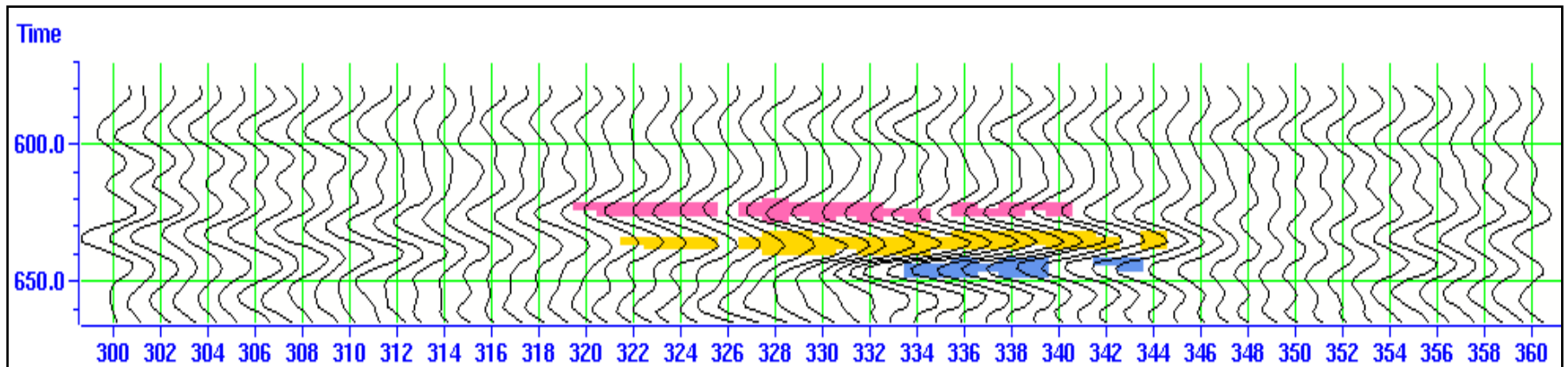
Intercept / Gradient Cross-Plots



Here is the cross-plot of Gradient and Intercept zones, where:

- Red = Top of Gas
- Yellow = Base of Gas
- Blue = Hard streak
- Ellipse = Mudrock trend

Below, the zones are plotted back on the seismic section.



- The second group of AVO methods, impedance methods, are based on the inversion of the reflectivity estimates to give impedance.
- The simplest set of methods use the reflectivity estimates from the Fatti et al. equation to invert for acoustic and shear impedance, and possibly density. That is:

$$R_{AI} \Rightarrow AI = \rho V_P \quad (\text{Acoustic Impedance})$$

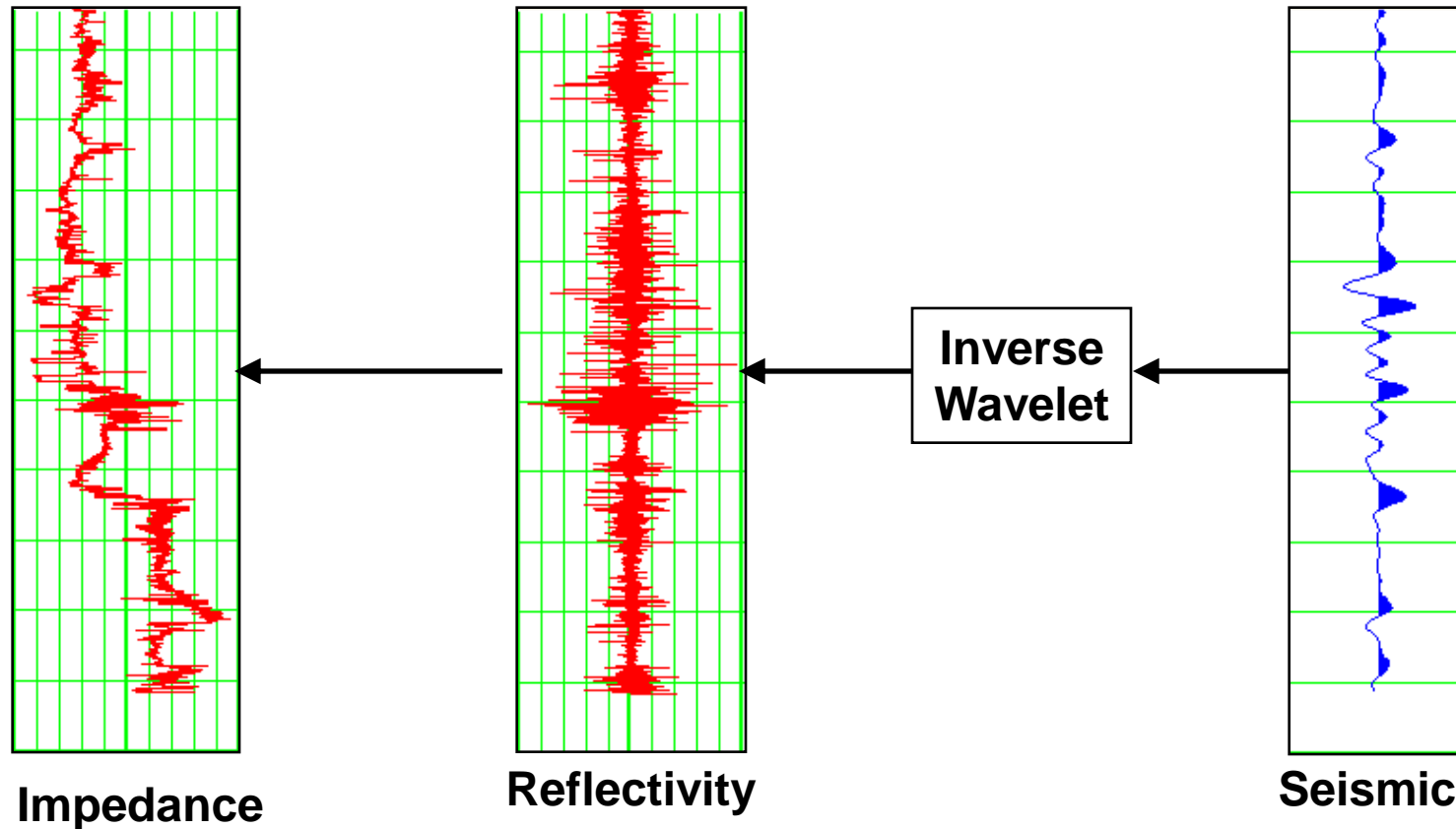
$$R_{SI} \Rightarrow SI = \rho V_S \quad (\text{Shear Impedance})$$

$$R_D \Rightarrow \rho \quad (\text{Density})$$

- The inversion can be done independently (separately for each term) or using simultaneous inversion.

Seismic inversion

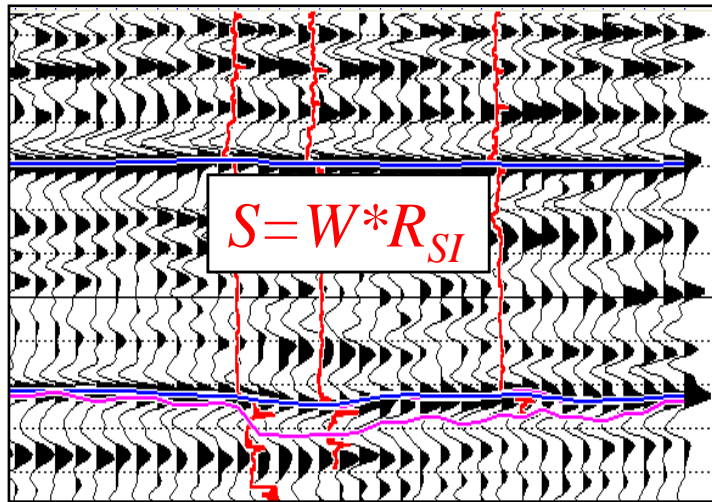
Seismic Inversion reverses the forward procedure:



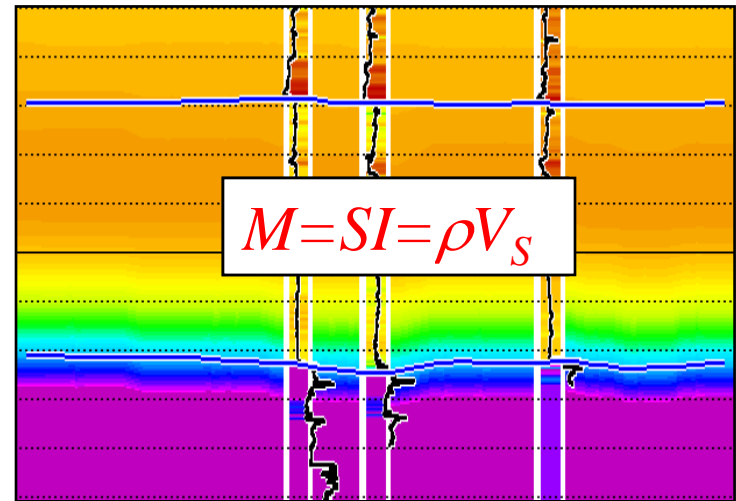
In principle, inversion is done as shown above, but in practice, the procedure is as shown in the next slide.

Model-based inversion

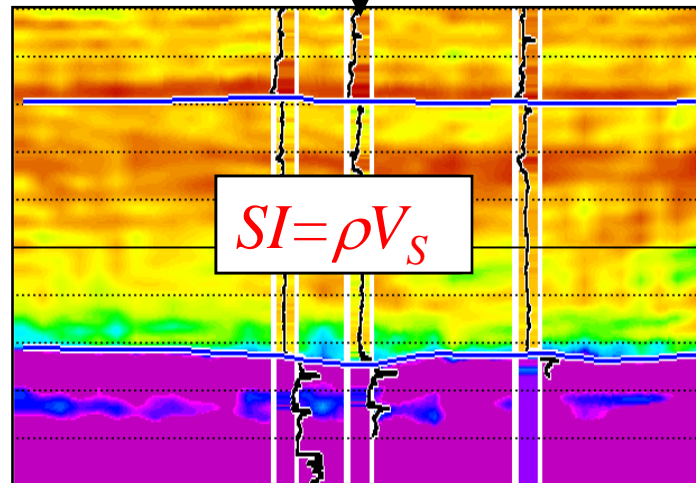
(1) Optimally process the seismic data



(2) Build model from picks and impedances



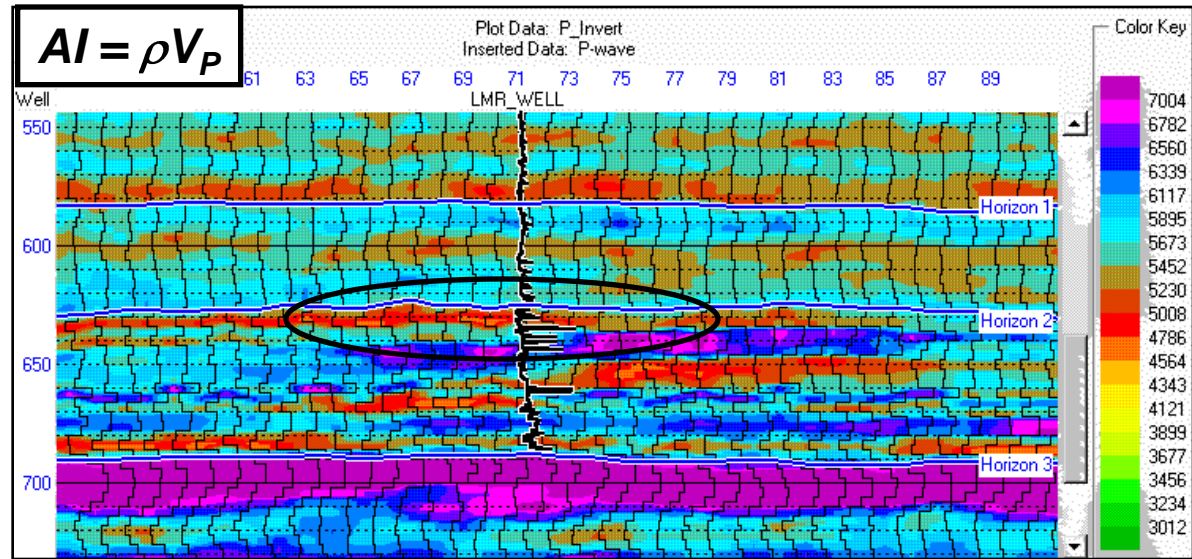
(3) Iteratively update model until output synthetic matches original seismic data.



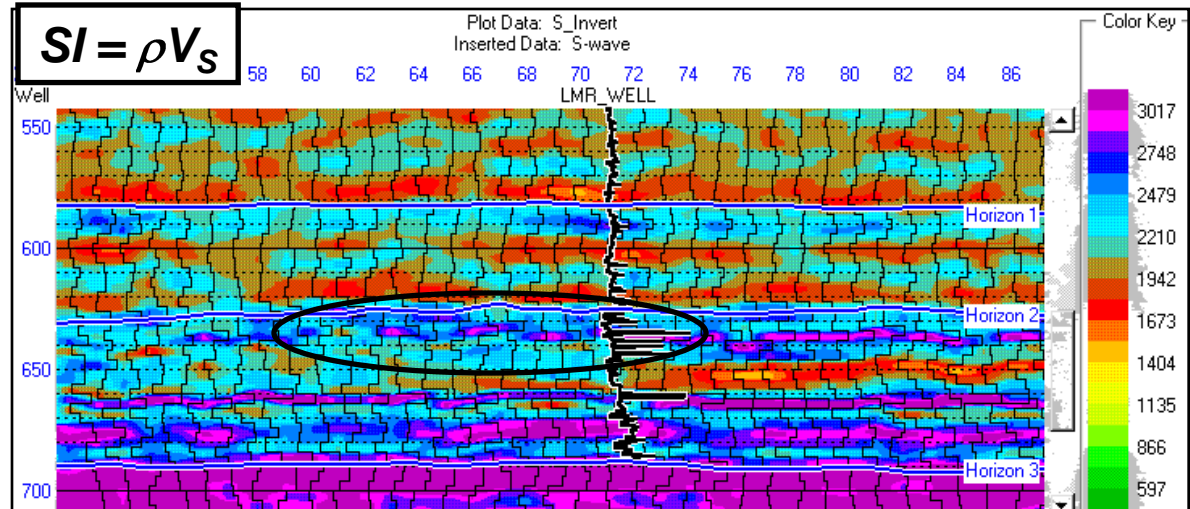
In shear impedance inversion the seismic, model and output are as shown here.

P-wave and S-wave Inversions

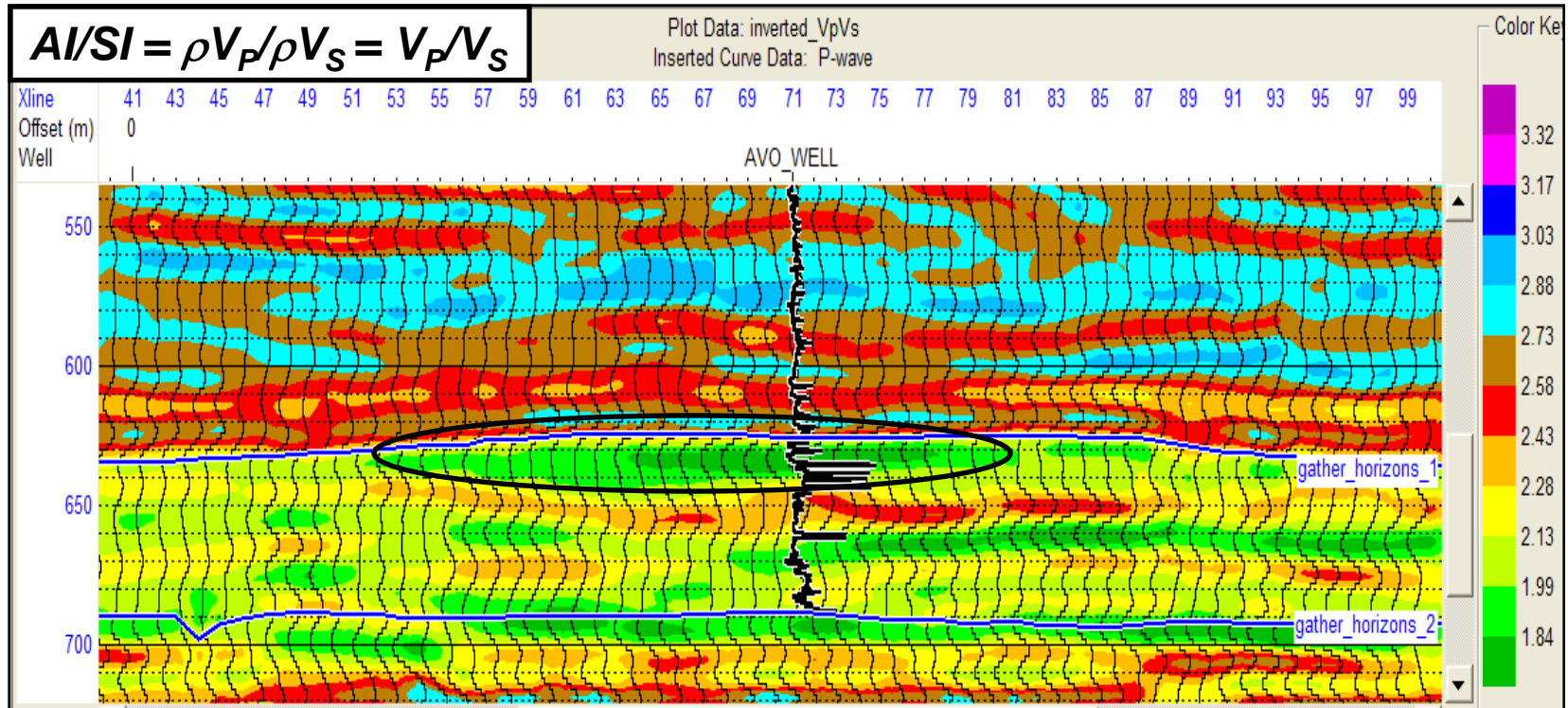
Here is the P-wave inversion result. The low acoustic impedance below Horizon 2 represents the gas sand.



Here is the S-wave inversion result. The gas sand is now an increase, since S-waves respond to the matrix.

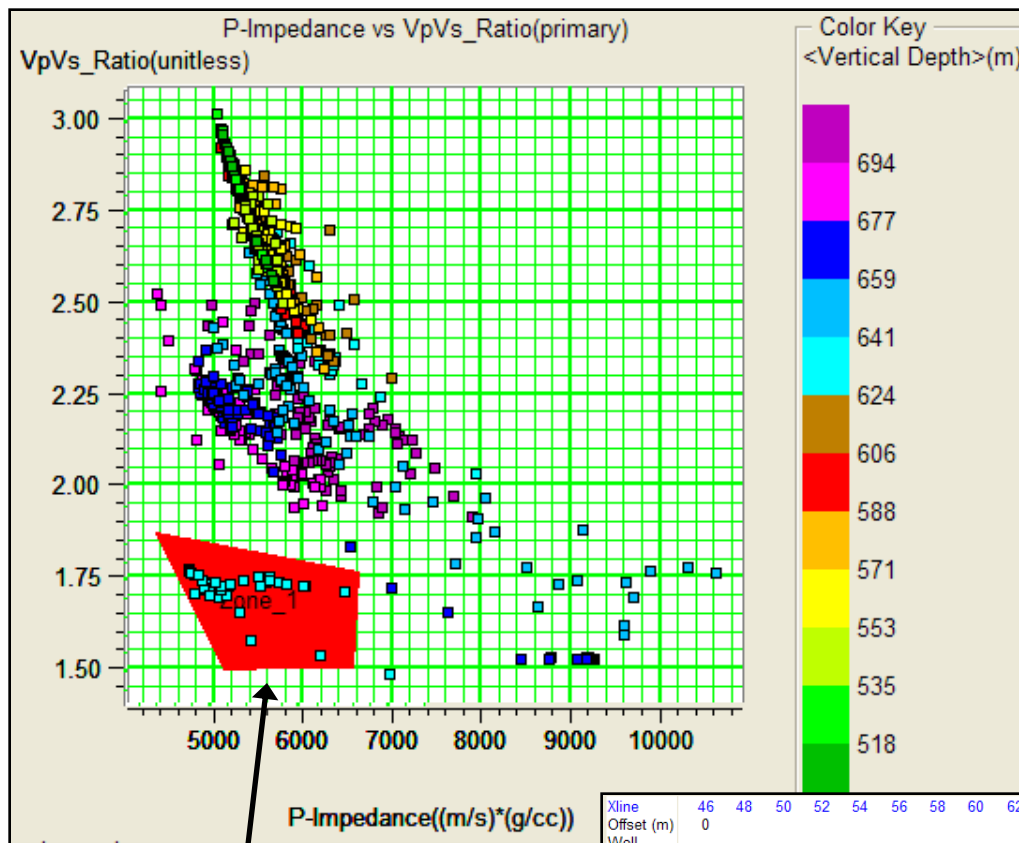


Vp/Vs Ratio



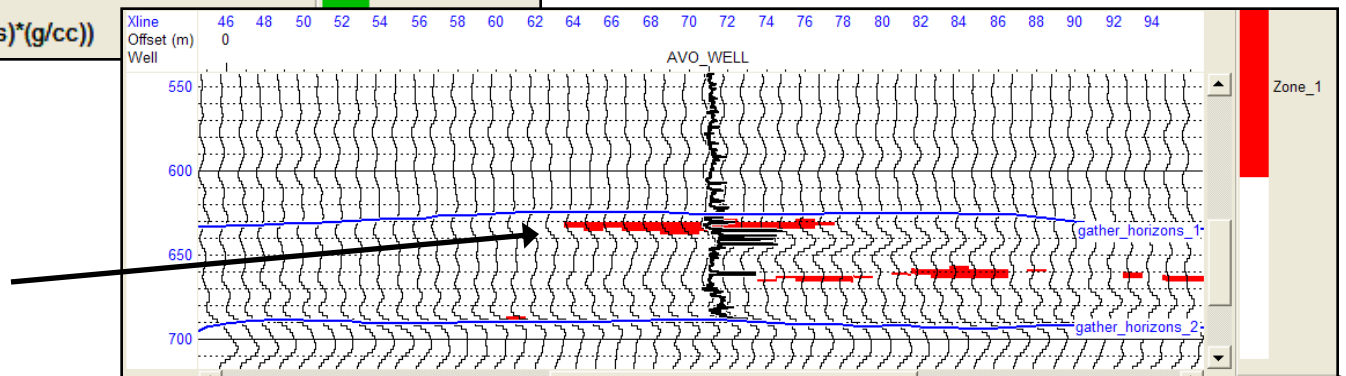
Here is the ratio of P to S impedance, which is equal to the ratio of P to S velocity. Notice the low ratio at the gas sand.

Cross-plot



When we crossplot V_P/V_S ratio against P-impedance, the zone of low values of each parameter should correspond to gas, as shown.

This zone should correspond to gas:



- Other AVO impedance methods combine the P and S -impedance volumes in new ways.
- For example, Goodway et al. (1997) proposed the Lambda-Mu-Rho (LMR) method which utilized the Lamé parameters λ and μ , and density, where it can be shown that:

$$\mu\rho = SI^2$$

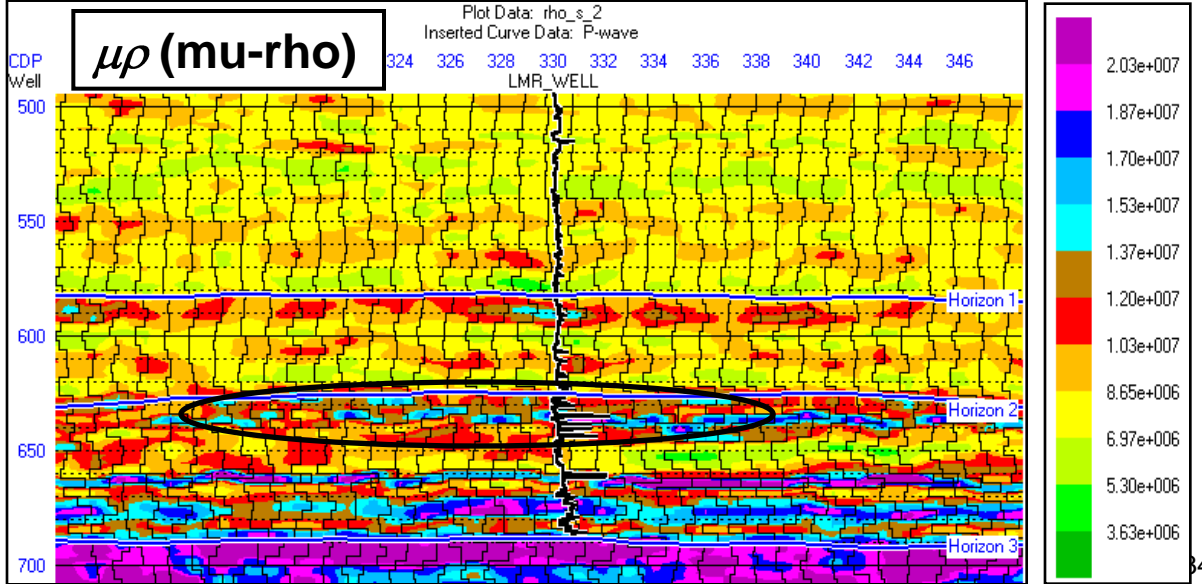
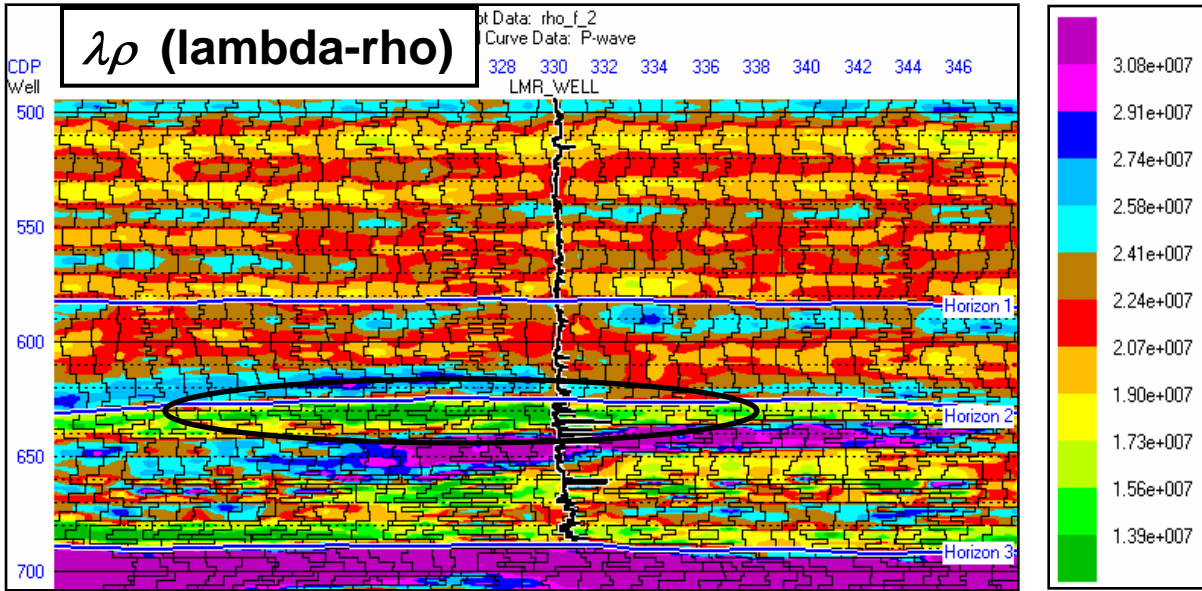
$$\lambda\rho = AI^2 - 2SI^2$$

- The interpretation of this approach is that $\mu\rho$ gives the matrix value of the rock and $\lambda\rho$ the fluid value.
- Russell et al. (2003) derived a more general approach based on Biot-Gassmann theory in which the factor 2 is replaced with $c = (V_P/V_S)_{dry}^2$, allowing empirical calibration to find a best value.

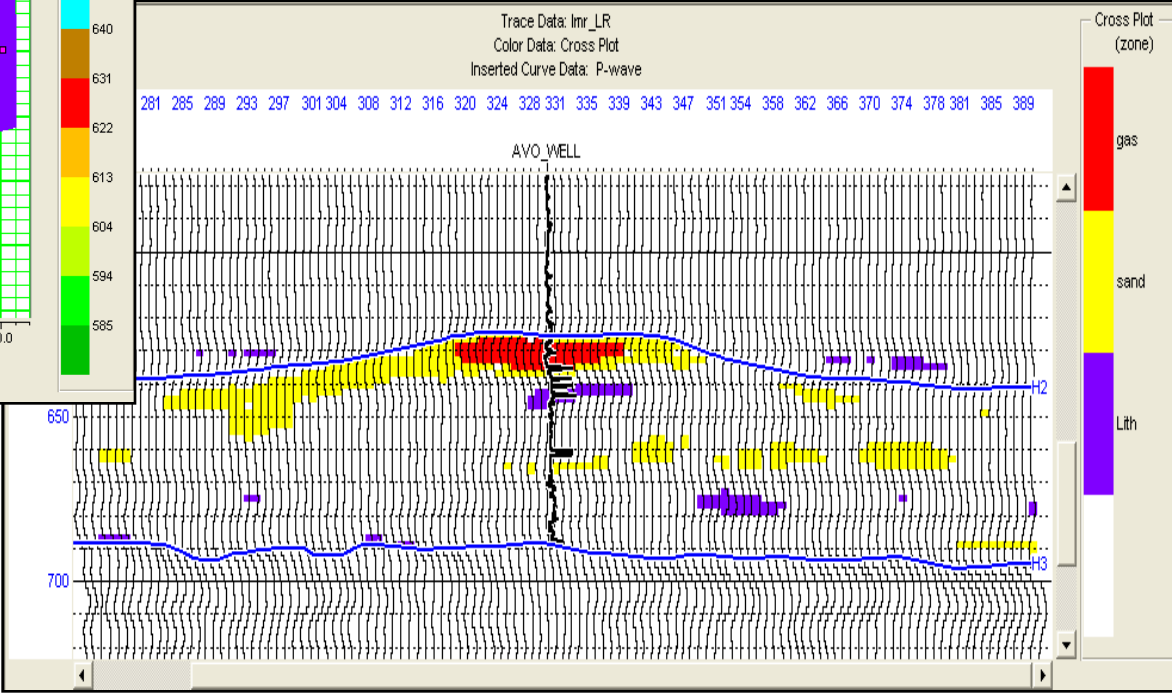
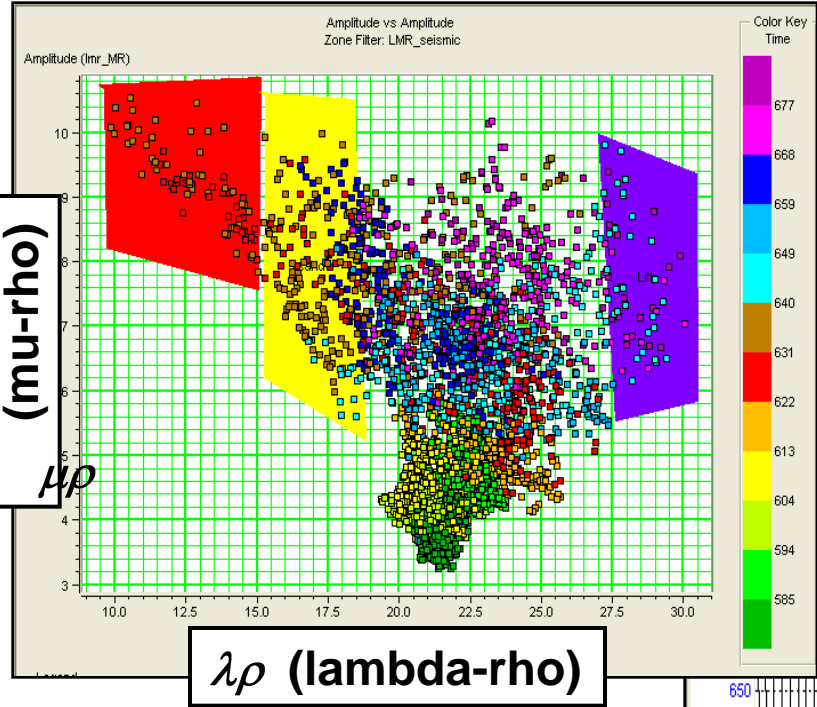
$\lambda\rho$ and $\mu\rho$ example

The $\lambda\rho$ and $\mu\rho$ sections derived from the AI and SI inverted sections shown earlier.

Note the decrease in $\lambda\rho$ and the increase in $\mu\rho$ at the gas sand zone.

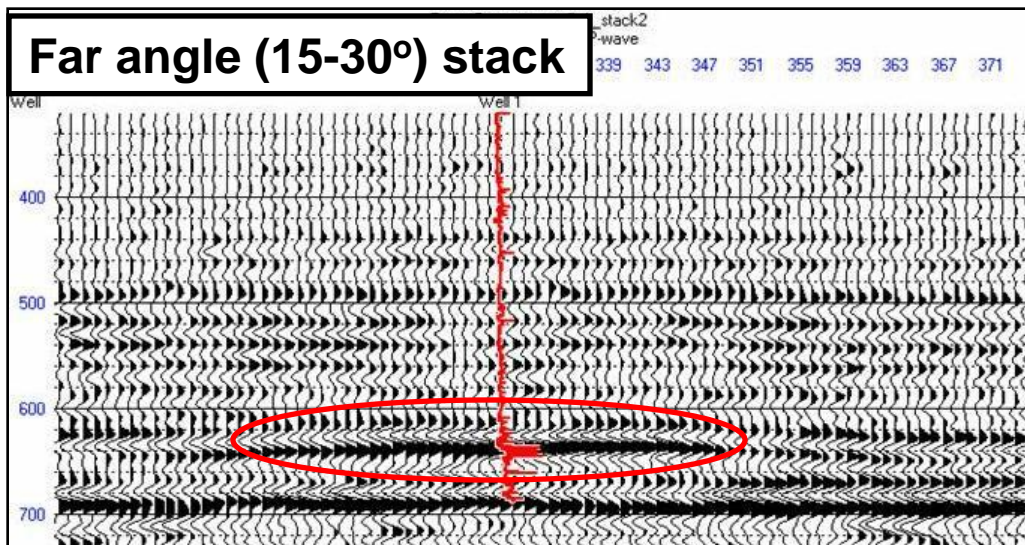
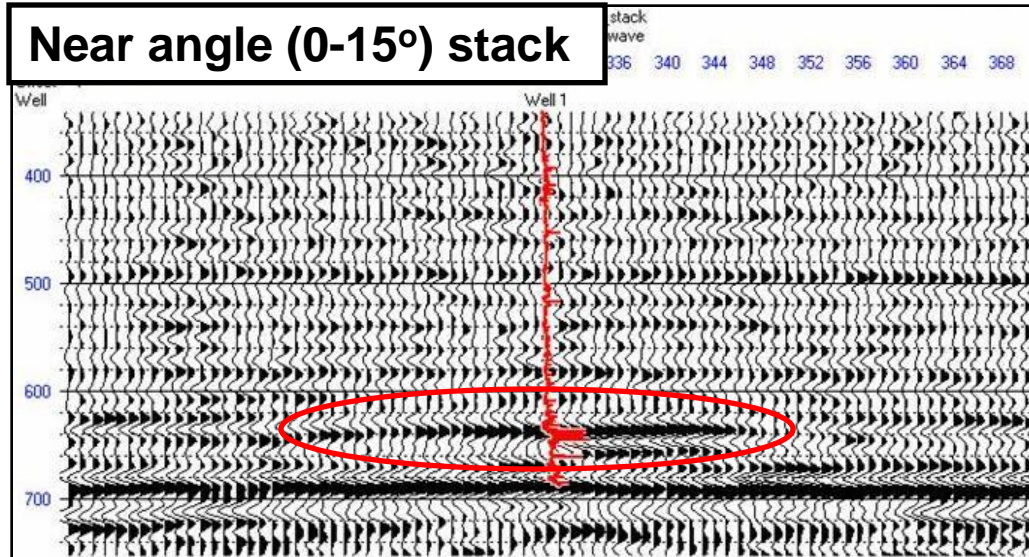


Colony Sand – cross-plot



A cross-plot of the $\lambda\rho$ and $\mu\rho$ sections, with the corresponding seismic section. Two zones are shown, where red = gas (low $\lambda\rho$ values) and blue = non-gas.

Near and far trace stacks



One AVO reflectivity method we did not discuss was near and far angle stacks, as shown here.

Note the amplitude of the “bright-spot” event is stronger on the far-angle stack than it is on the near-angle stack.

But what does this mean?

Elastic Impedance

- The equivalent impedance method to near and far angle stacking is Elastic Impedance, or EI (Connolly, 1999).
- To understand EI , recall the Aki-Richards equation:

$$R_p(\theta) = a \frac{\Delta V_P}{2V_P} + b \frac{\Delta V_S}{2V_S} + c \frac{\Delta \rho}{2\rho}, \text{ where :}$$

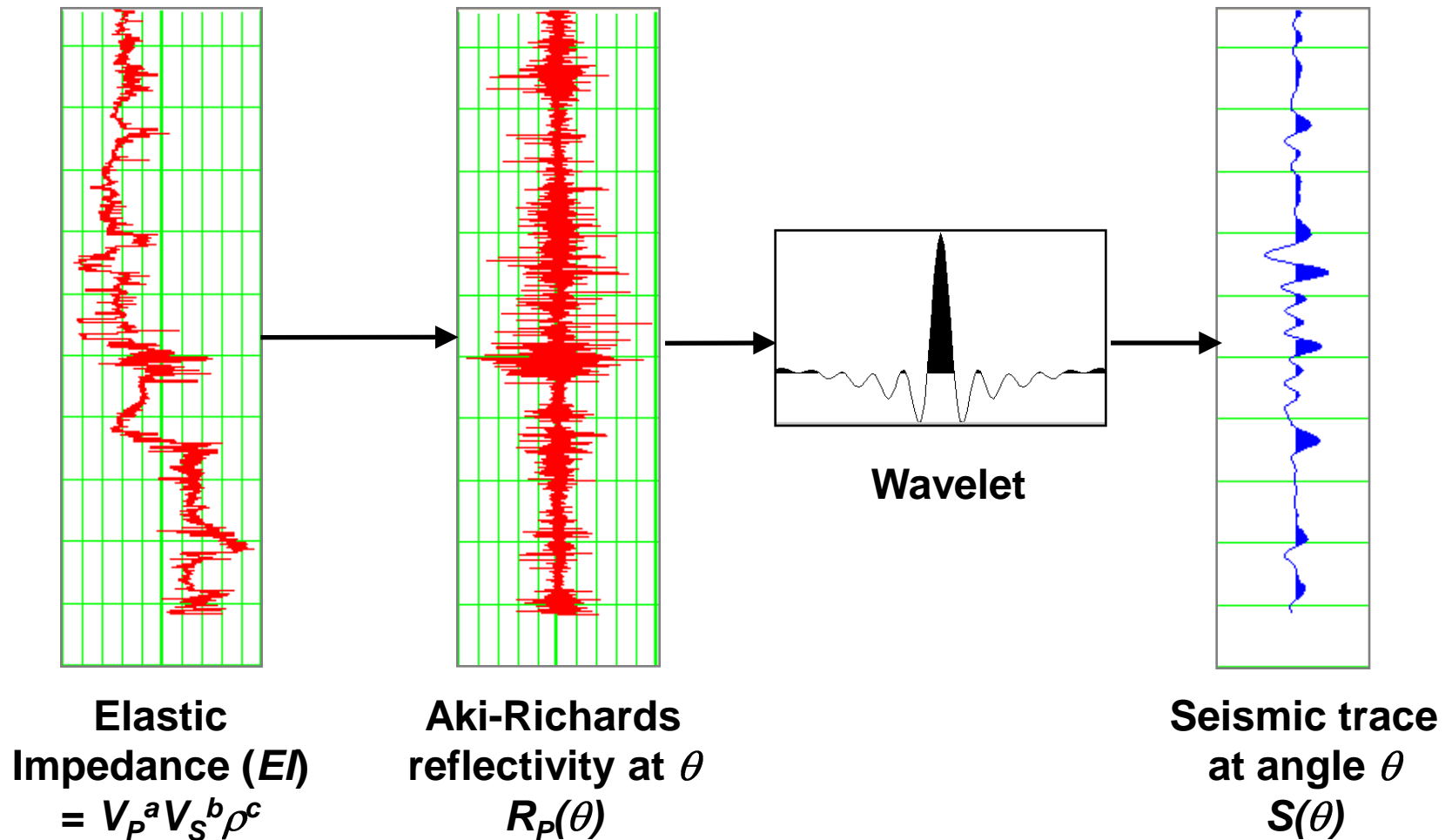
$$a = 1 + \tan^2 \theta, \quad b = -8K \sin^2 \theta, \quad \text{and} \quad c = 1 - 2K \sin^2 \theta.$$

- Connolly postulated that associated with this equation is an underlying elastic impedance, written (where I have re-named the reflectivity to match the EI concept):

$$R_{EI}(\theta) = \frac{1}{2} \frac{\Delta EI(\theta)}{EI(\theta)} \approx \frac{1}{2} \Delta \ln EI(\theta), \text{ where } EI(\theta) = V_P^a V_S^b \rho^c$$

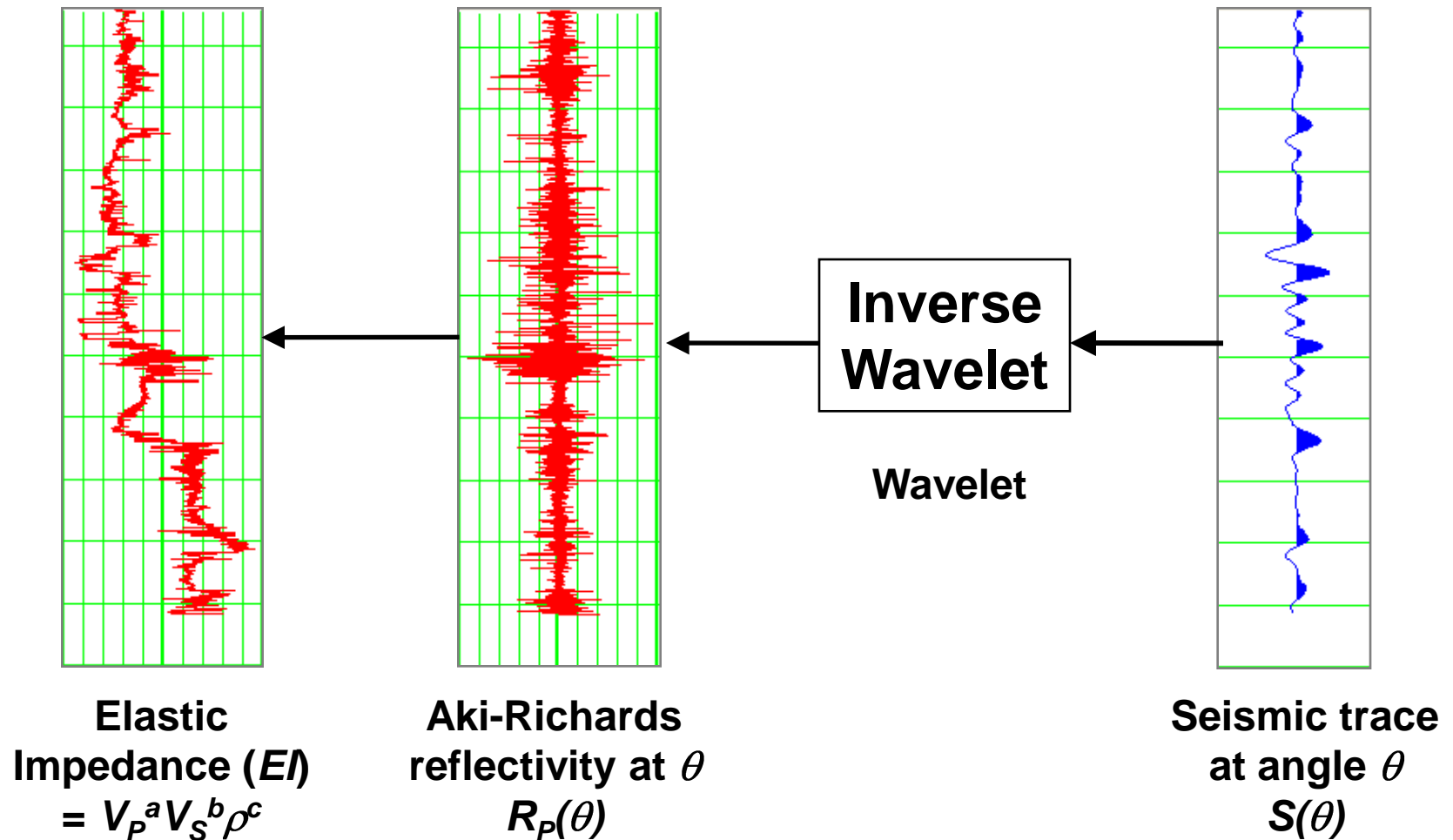
The elastic impedance model

Analogous to AI , the model that forms the basis for EI is:



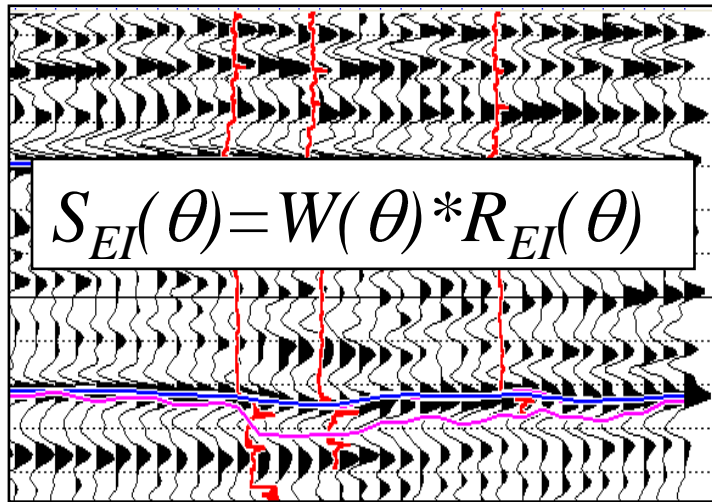
The elastic impedance model

Elastic impedance inversion reverses the forward EI model:

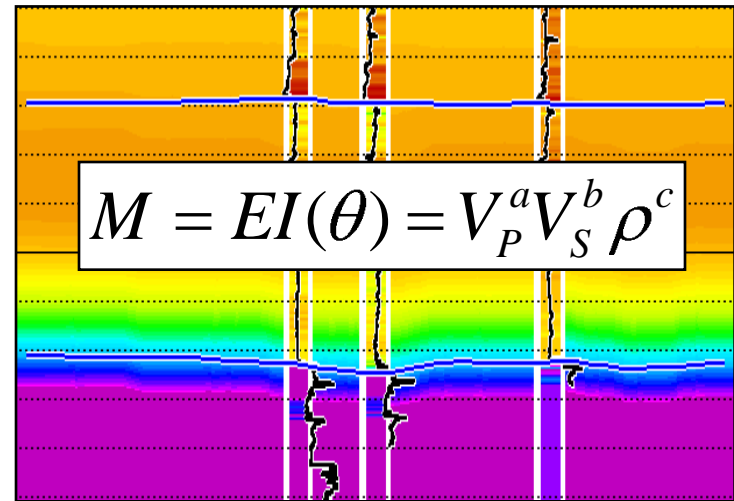


Elastic impedance inversion

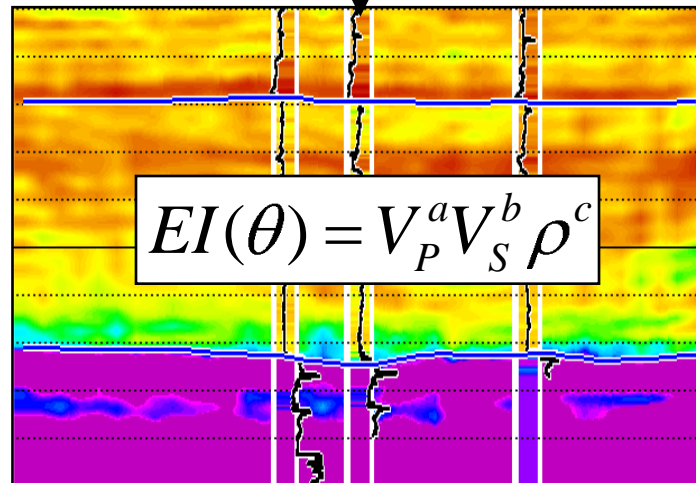
(1) Optimally process the seismic data



(2) Build model from picks and impedances



(3) Iteratively update model until output synthetic matches original seismic data.

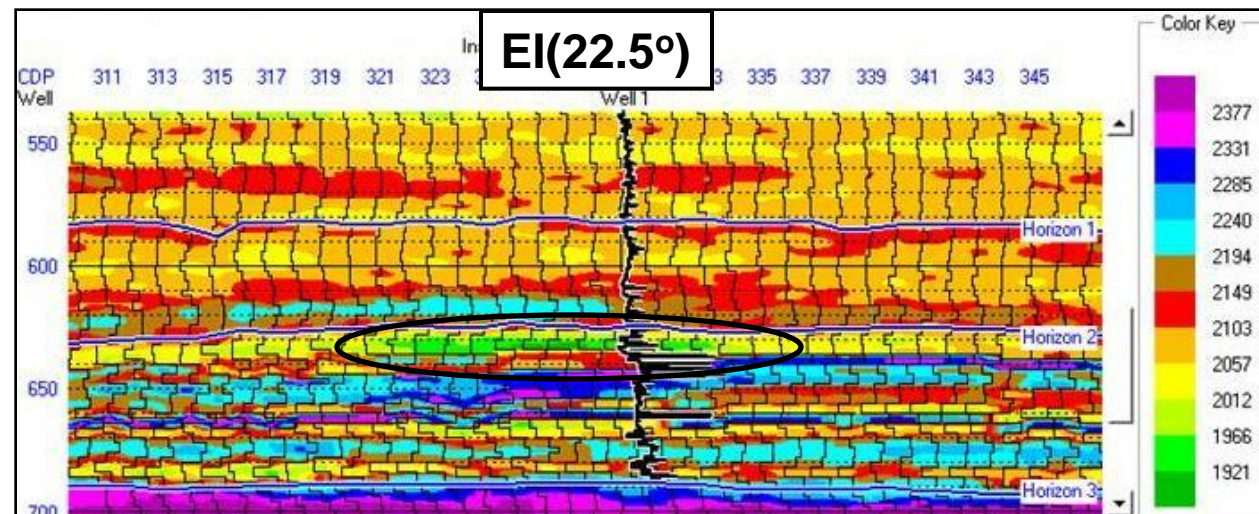
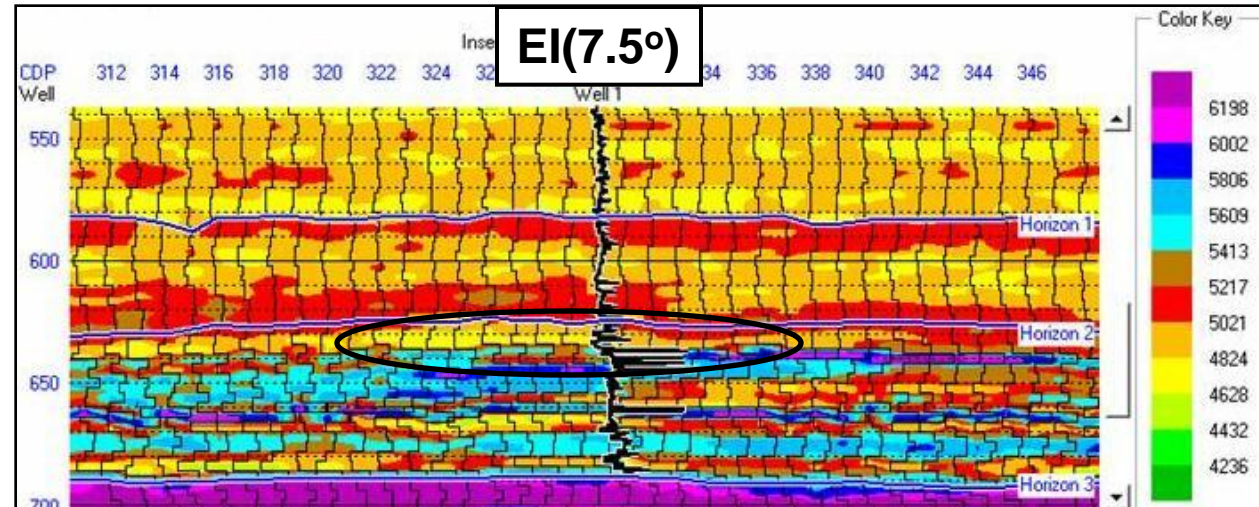


In elastic impedance inversion the seismic, model and output are as shown here.

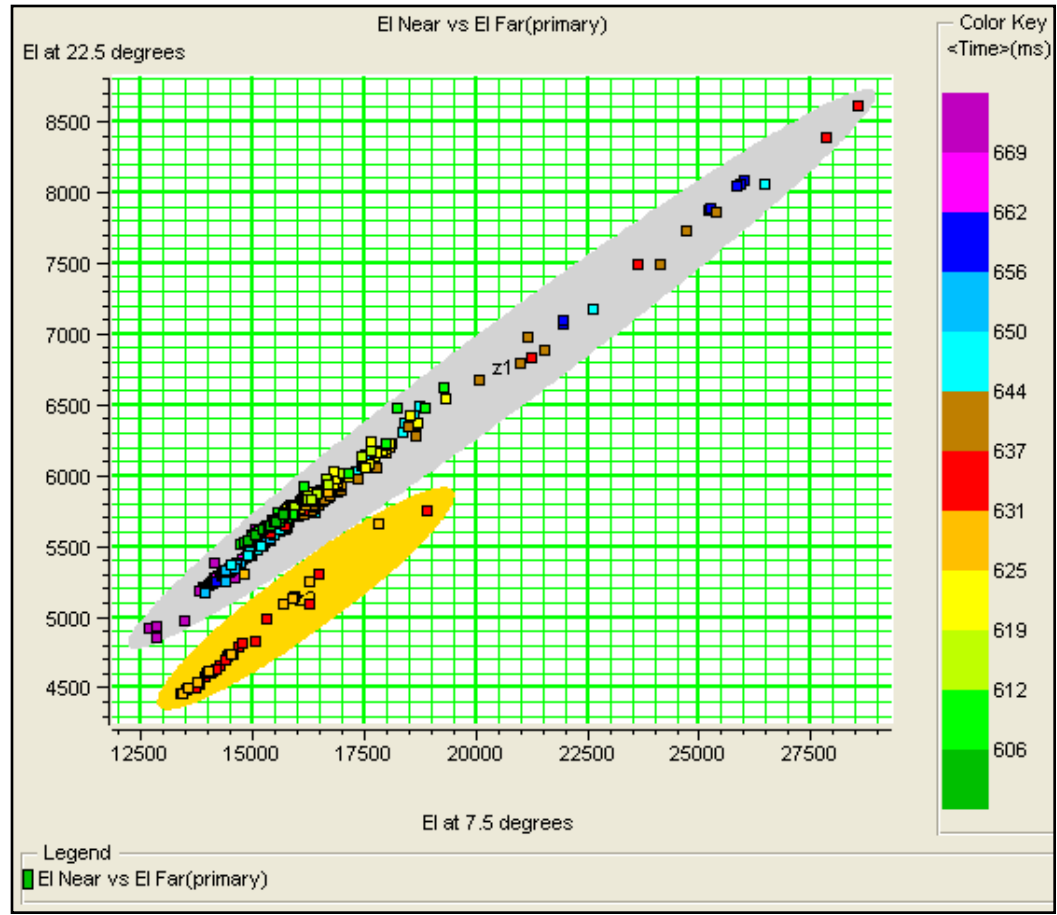
Gas sand case study

Here is the comparison between the *EI* inversions of the near-angle stack and far-angle stack.

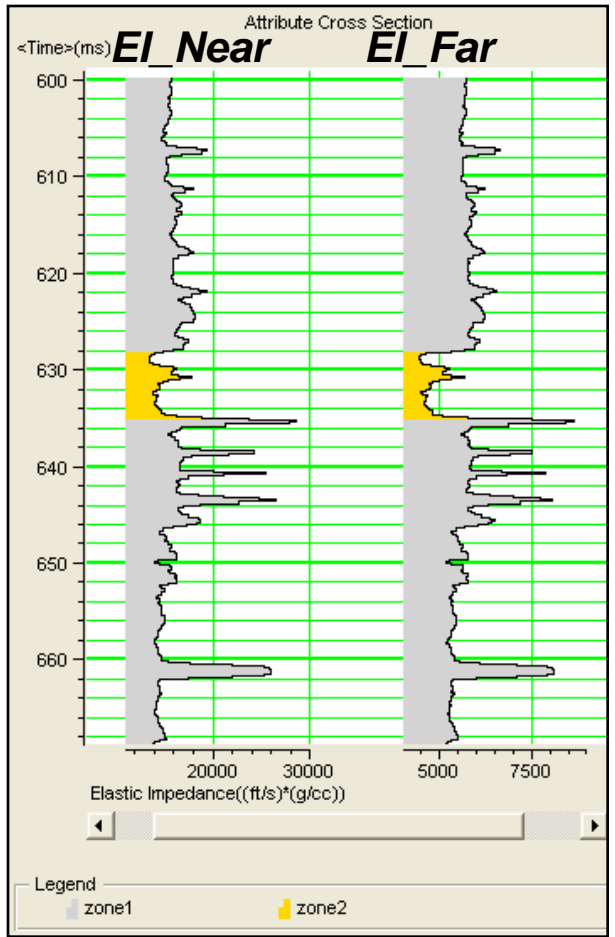
Notice the decrease in the elastic impedance value on the far-angle stack.



EI from logs



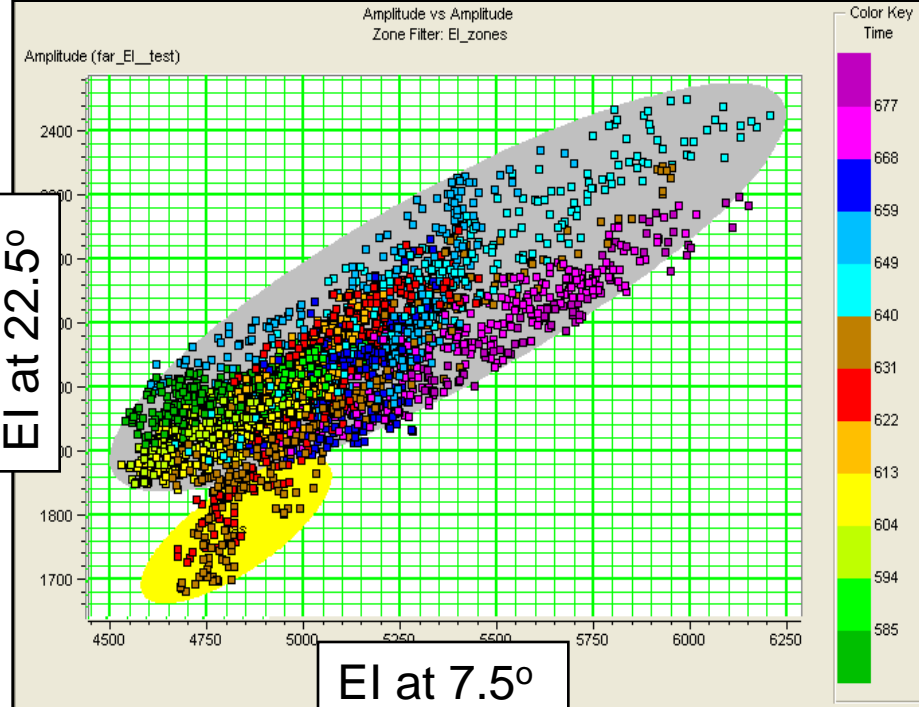
(a)



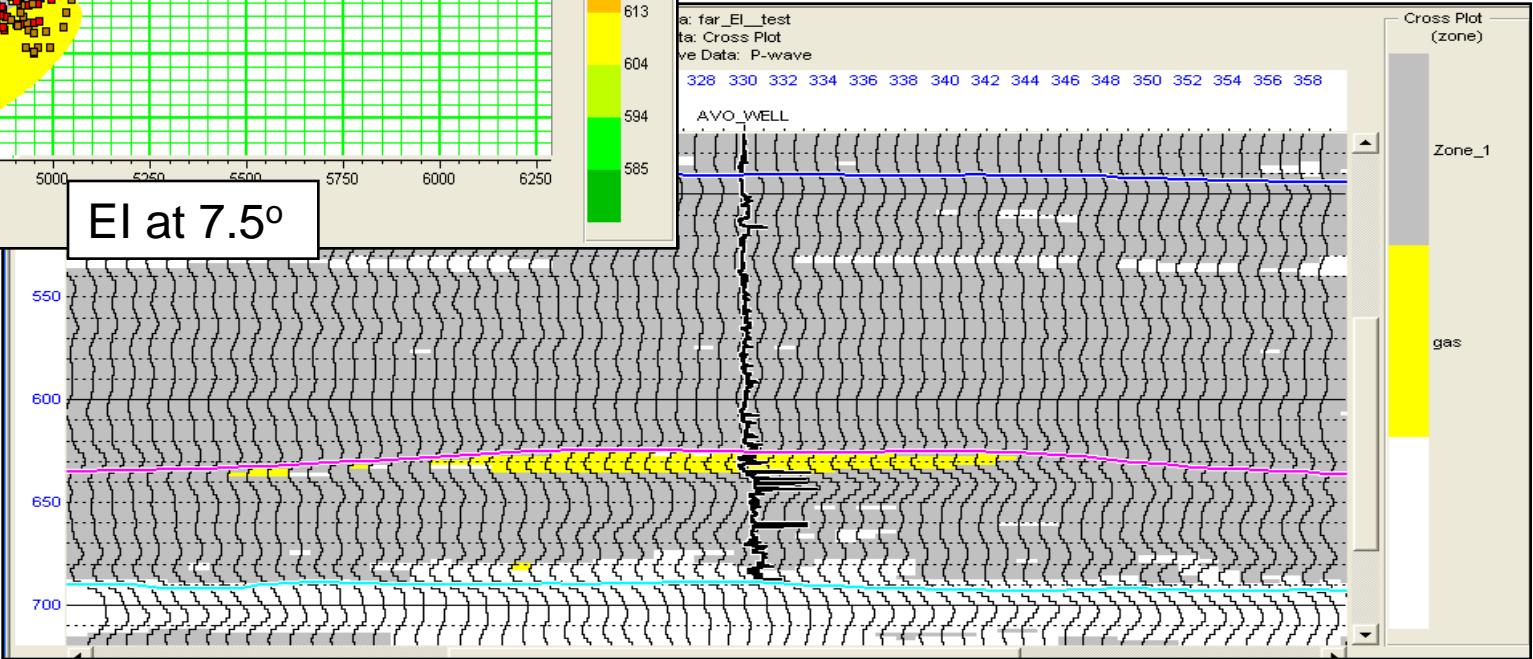
(b)

The figures show the (a) crossplot between near and far *EI* logs, and (b) the zones on the logs. Notice the clear indication of the gas sand (yellow).

Gas sand case study

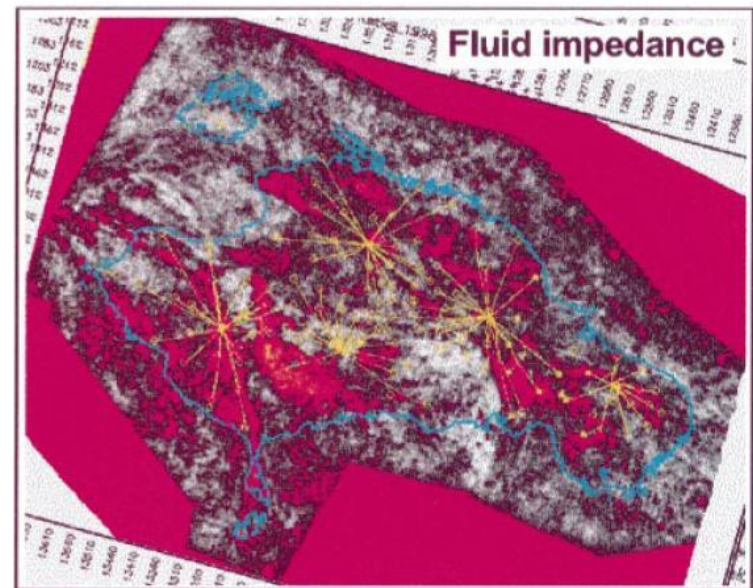
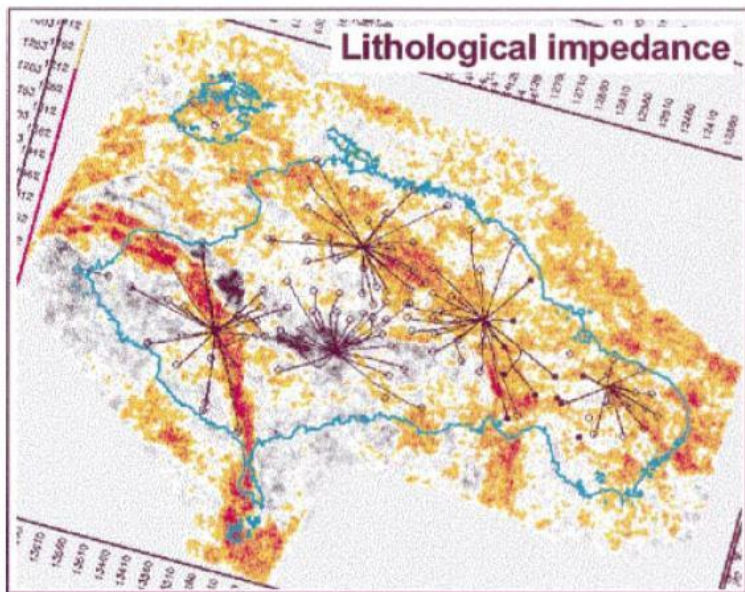


This figure shows a crossplot between EI at 7.5° and EI at 22.5°. The background trend is the grey ellipse, and the anomaly is the yellow ellipse. As shown below, the yellow zone corresponds to the known gas sand.



Extended Elastic Impedance (EEI)

- Since EI values do not scale correctly for different angles, Whitcombe et al. (2002) created a new method (EEI) that did scale correctly, and was extended to predict other rock physics and fluid parameters (using the χ factor).
- We will not go into the details today, but here is an example of lithology and fluid extraction from a 3D dataset:



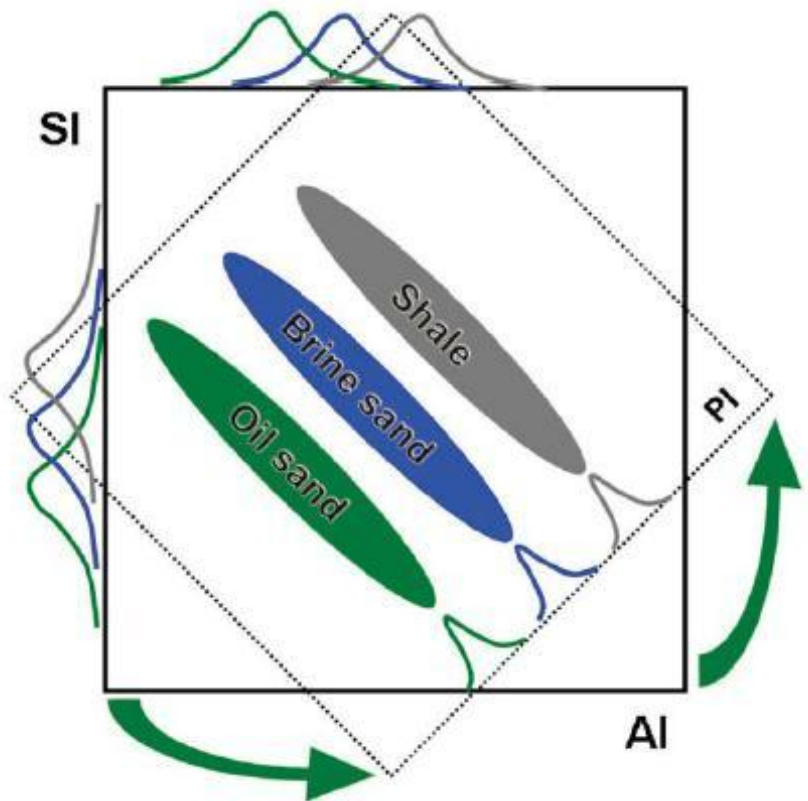
- Finally, Quackenbush et al. (2006) proposed the Poisson Impedance (*PI*) attribute, given by:

$$PI = AI - cSI, \text{ where } c = \sqrt{2}$$

- The authors show that Poisson Impedance is like a scaled version of the product of Poisson's ratio and density.
- We can think of this method as an impedance version of Poisson Reflectivity, defined by Smith and Gidlow.
- Also note the relationship with $\lambda\rho$:

$$\lambda\rho = AI^2 - 2SI^2 = \left(AI + \sqrt{2}SI \right) \left(AI - \sqrt{2}SI \right) = \left(PI + 2\sqrt{2}SI \right) PI$$

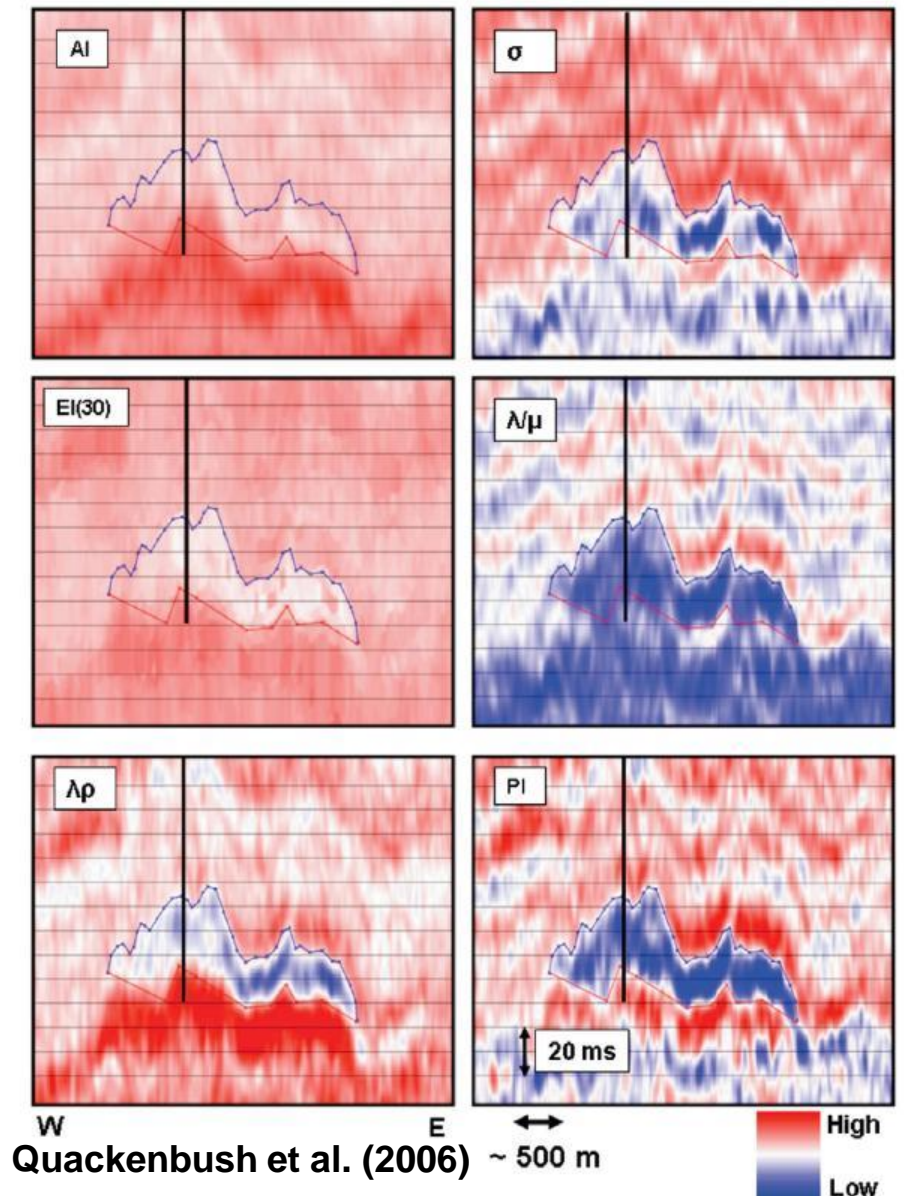
Poisson Impedance (PI)



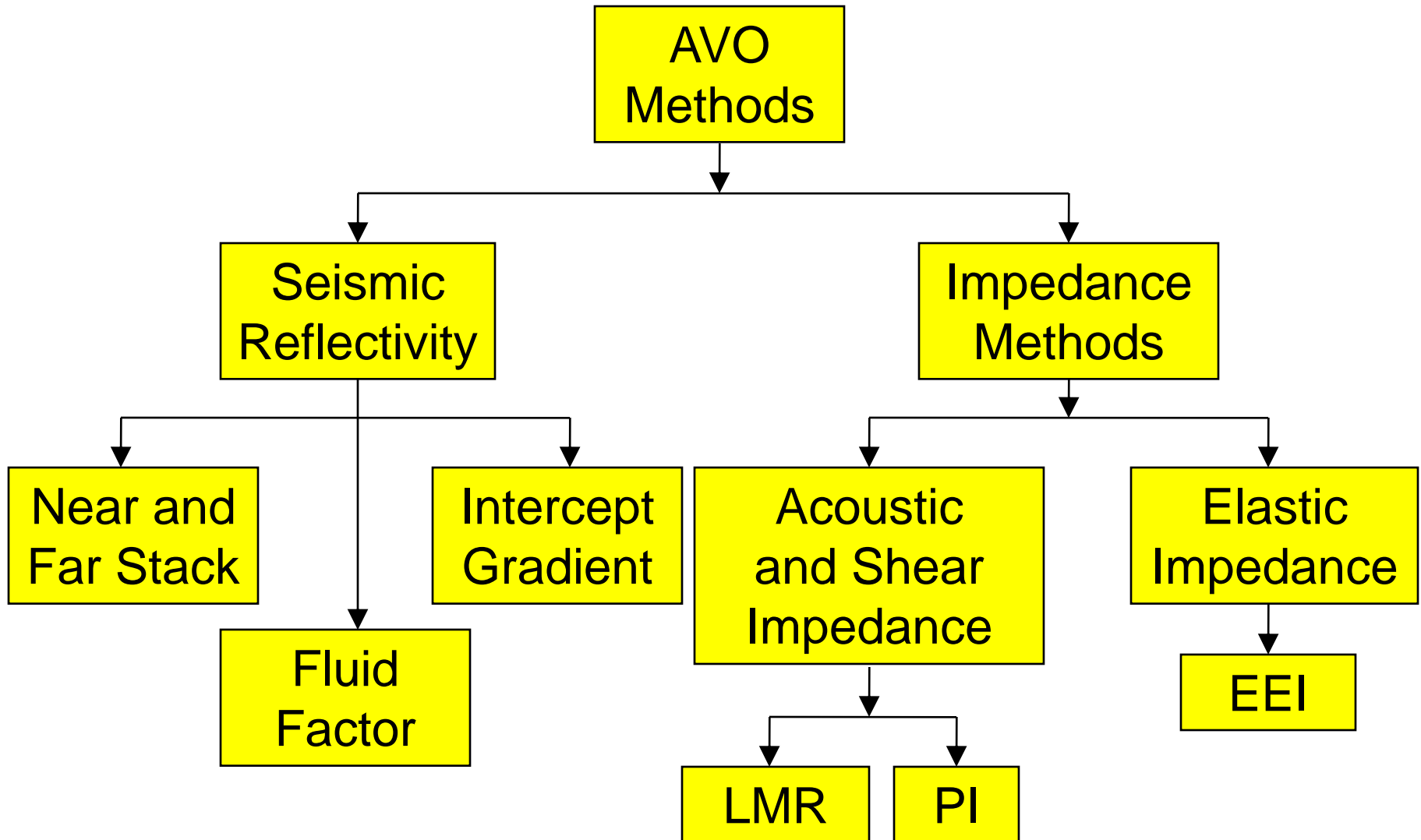
Quackenbush et al. (2006)

Above, notice that PI can be thought of as a rotation in *AI/SI* space.

On the right is a comparison of *PI* with other impedance attributes.



Summary of AVO methods



- The advantages of AVO methods based on seismic reflectivity are that:
 - They are robust and easy to derive.
 - They allow the data to “speak for itself” since their interpretation relies on detecting deviations away from a background trend.
- The disadvantage of AVO methods based on seismic reflectivity is that:
 - They do not give geologists what they really want, which is some physical parameter with a trend.

- The advantages of AVO and inversion methods based on impedance are that:
 - They give geologists what they want: a physical parameter with a trend.
 - They can be transformed to reservoir properties.
- The disadvantages of AVO and inversion methods based on impedance are as follows:
 - The original data has to be transformed from its natural reflectivity form.
 - Care must be taken to derive a good quality inversion.

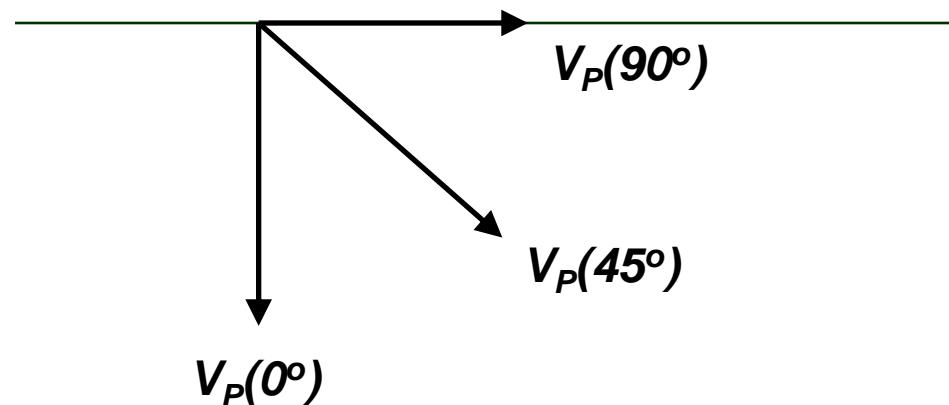
- This presentation has been a brief overview of the various methods used in Amplitude Variations with Offset (AVO) and pre-stack inversion.
- I showed that all of these methods are based of the Aki-Richards approximation to the Zoeppritz equations.
- I then subdivided these techniques as either:
 - (1) seismic reflectivity or (2) impedance methods.
- Seismic reflectivity methods are straightforward to derive and to interpret but do not give us physical parameters.
- Impedance methods are more difficult to derive but give us physical parameters including reservoir properties.
- In the final analysis, there is no single “best” method for solving all your exploration objectives. Pick the method that works best in your area.

Acknowledgements

- I wish to thank my colleagues Dan Hampson and Graham Carter for their many suggestions that improved this presentation.
- Also I would like to thank Fred Hilterman, John Castagna, Leon Thomsen, George Smith and Maurice Gidlow for their ground-breaking papers on AVO and anisotropy and my inspiring discussions with each of them over the years.

Appendix: Anisotropic effects

- Let us finish with a discussion of anisotropic effects.
- In an isotropic earth P and S-wave velocities are independent of angle.
- In an anisotropic earth, velocities and other parameters are dependent on direction, as shown below.



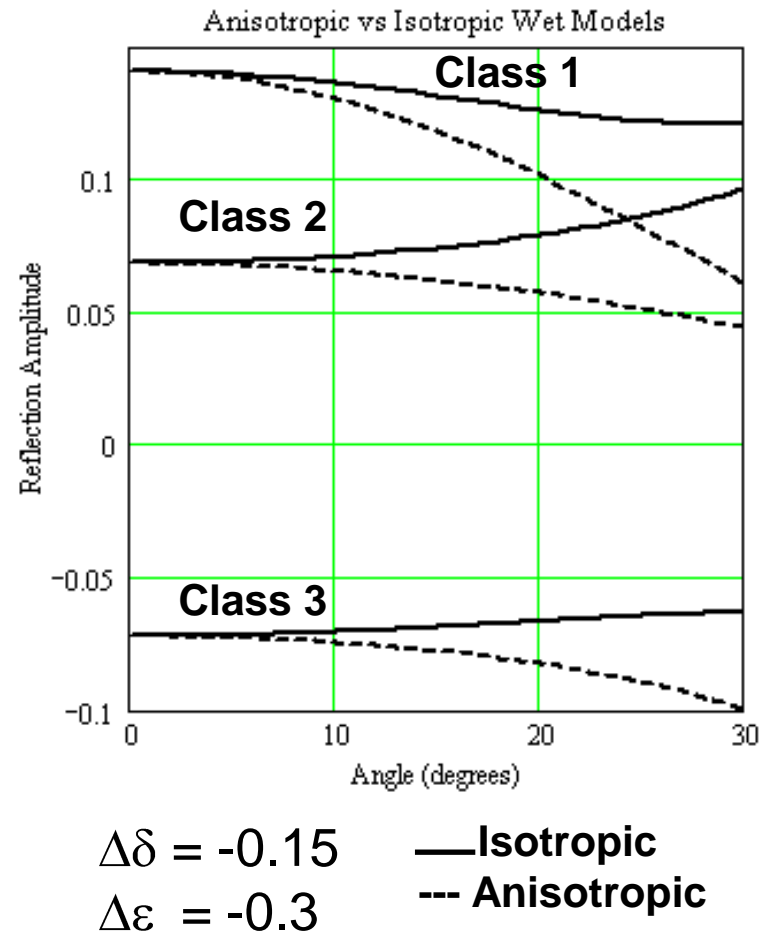
- We will consider the cases of *Transverse Isotropy* with a *vertical* symmetry axis, or *VTI*, and *Transverse Isotropy* with a *Horizontal* symmetry axis, or *HTI*.

VTI – AVO Effects

The VTI model consists of horizontal layers and can be extrinsic, caused by fine layering of the earth, or intrinsic, caused by particle alignment as in a shale. It can be modeled as follows, where $\Delta\delta$ and $\Delta\varepsilon$ are the change in Thomsen's first two anisotropic parameters across a boundary:

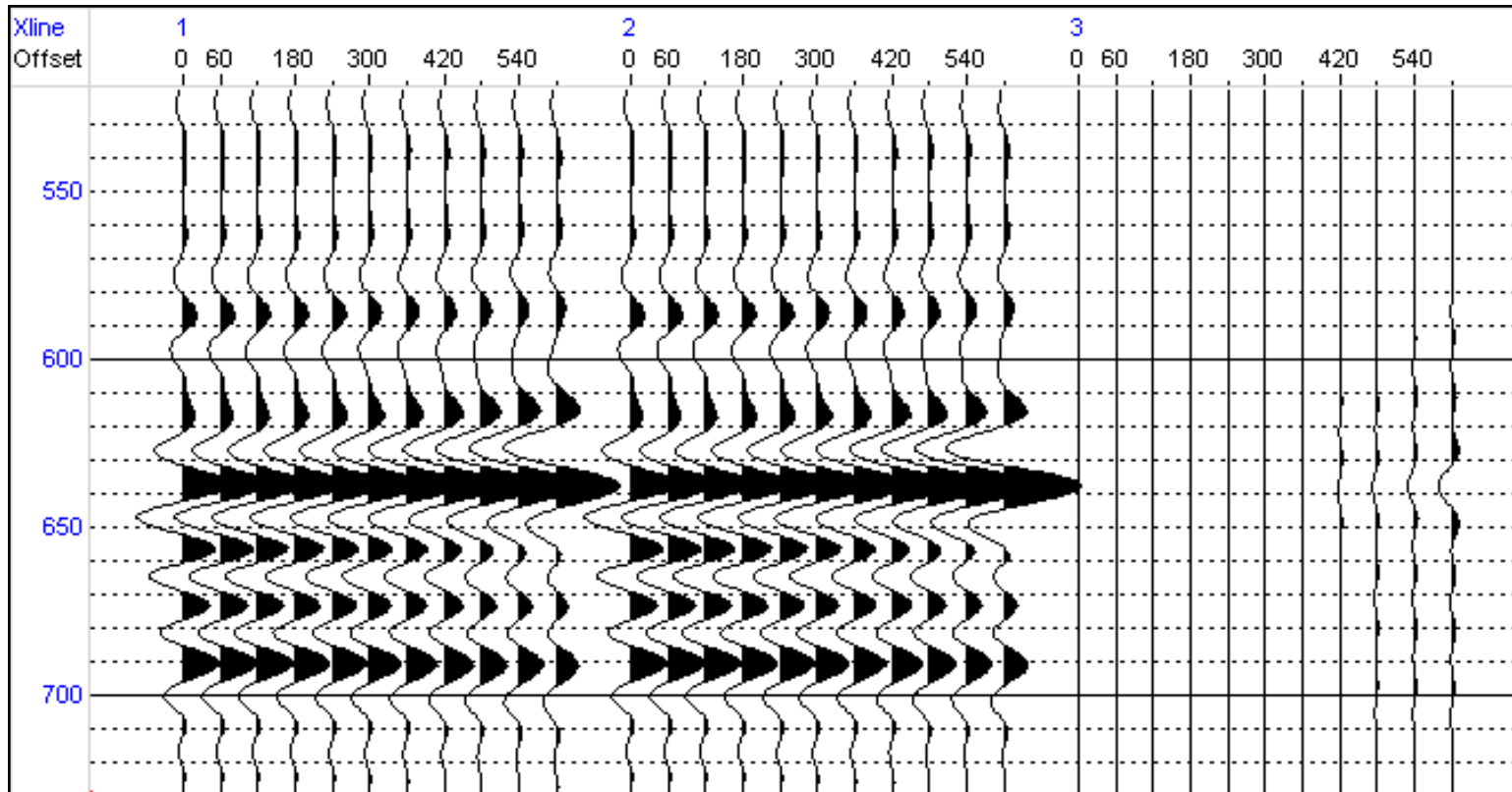
$$R_{VTI}(\theta) = A + \left(B + \frac{\Delta\delta}{2} \right) \sin^2 \theta$$
$$\dots + \left[C + \frac{\Delta\varepsilon}{2} \right] \sin^2 \theta \tan^2 \theta$$

A VTI shale over an isotropic wet sand can create the appearance of a gas sandstone anomaly, as shown here:



Adapted from Blangy (1997)

Anisotropic AVO Synthetics



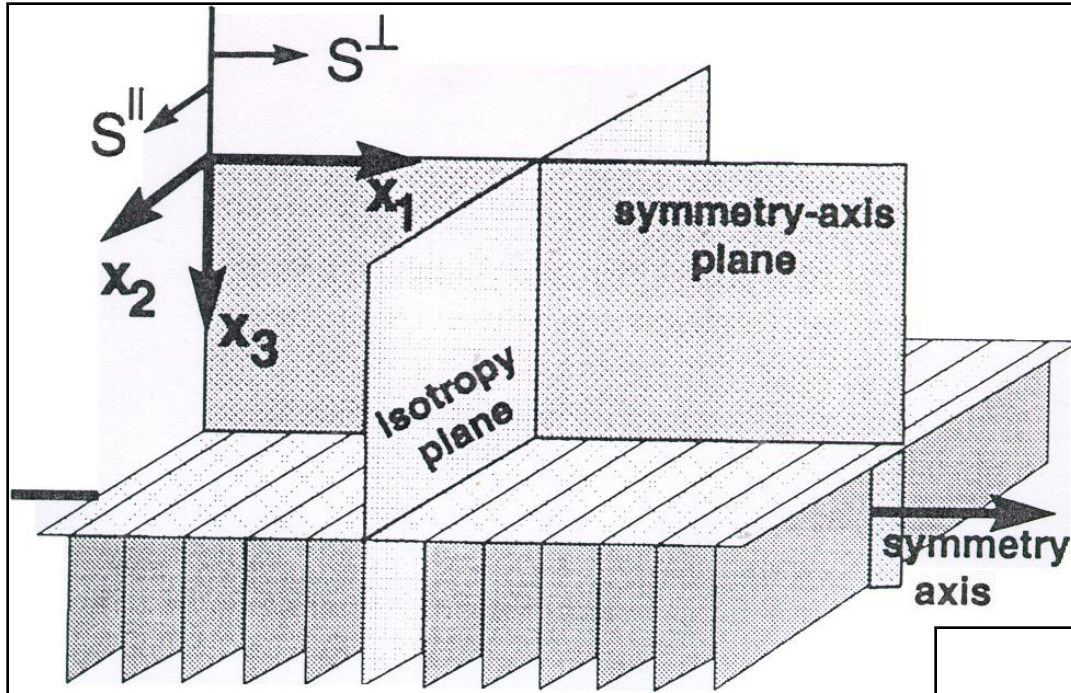
(a) Isotropic

(b) Anisotropic

(a) - (b)

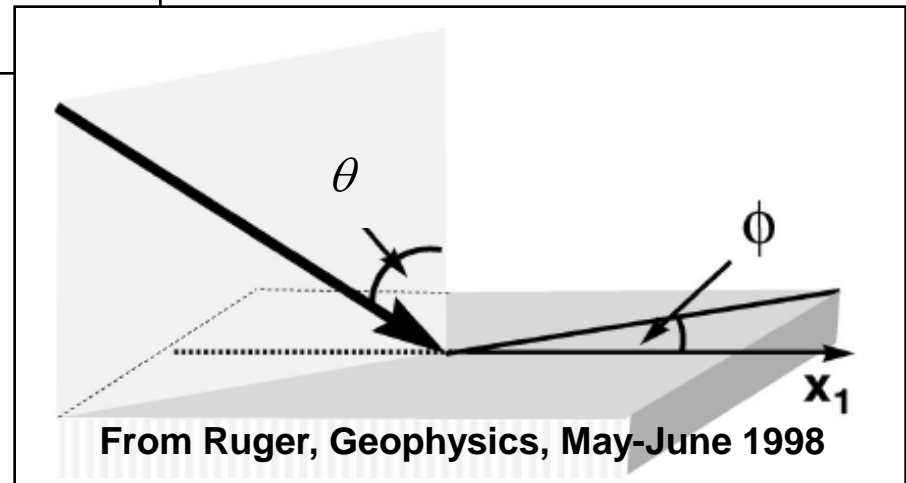
In this display, the synthetic responses for a shallow gas sand in Alberta are shown. Note the difference due to anisotropy.

HTI effects on AVO



Next, we will discuss AVO and HTI anisotropy, as shown in the figure on the left. This shows a set of fractures, with the symmetry axis orthogonal to the fractures, and the isotropy plane parallel to the fractures.

In addition to the raypath angle θ , we now introduce an azimuth angle ϕ , which is defined with respect to the symmetry-axis plane. Note that the azimuth angle ϕ is equal to 0 degrees along the symmetry-axis plane and 90 degrees along the isotropy plane.



Modeling HTI

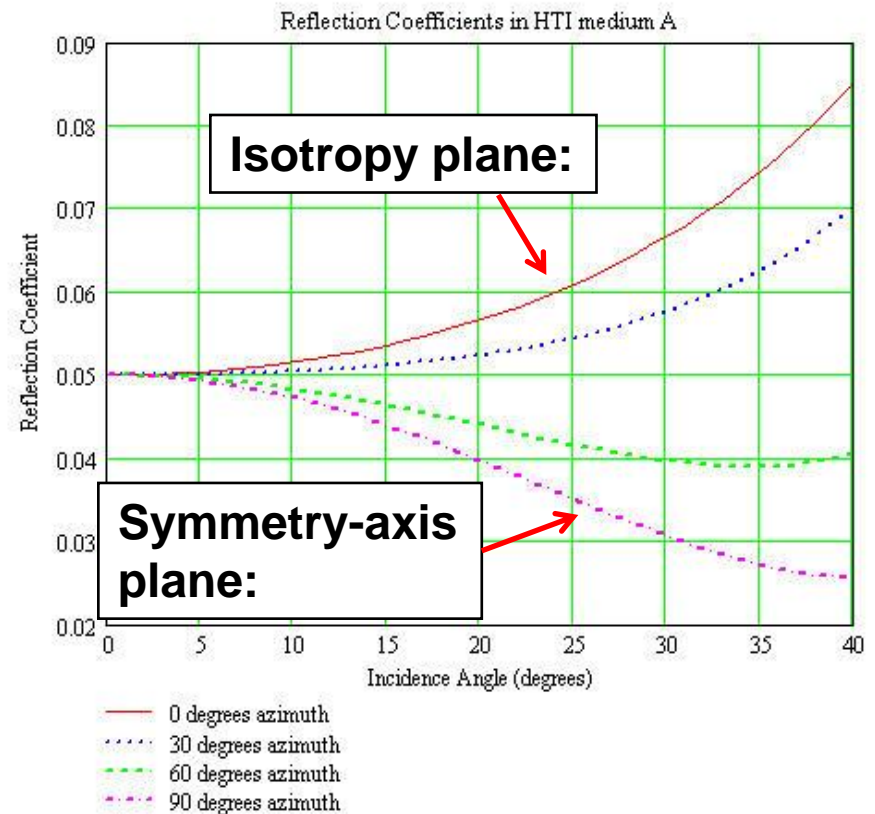
HTI anisotropy can be modeled with the following equation, where γ is Thomsen's third anisotropic parameter and (V) indicates with respect to vertical. When $\phi = 0$, along the isotropy plane, we get the isotropic equation, as expected:

$$R_{HTI} = A + B + B_{HTI} \cos^2 \phi \sin^2 \theta + \dots + C + C_{HTI} \cos^2 \phi \sin^2 \theta \tan^2 \theta$$

where :

$$B_{HTI} = \frac{1}{2} \left[\Delta \delta^{(V)} + 8 \left[\frac{V_S}{V_P} \right]^2 \Delta \gamma \right],$$

$$C_{HTI} = \frac{1}{2} \left[\Delta \delta^{(V)} \sin^2 \phi - \Delta \varepsilon^{(V)} \right]$$



The reflection coefficients for a model where only γ changes, as a function of incidence angle for 0, 30, 60 and 90 degrees azimuth.

Fracture Interpretation

AVO Fracture Analysis measures fracture volume from differences in AVO response with Azimuth. Fracture strike is determined where this difference is a maximum.

Direction of Line is estimated fault strike, length of line and color is estimated crack density

